

Journal Pre-proof

A study in analytical chemistry of adsorption of heavy metal ions using chitosan/graphene nanocomposites

H.N.K. AL-Salman, Marwa sabbar Falih, Hiba B. Deab, Usama S. Altimari, Hussein Ghafel Shakier, Ashour H. Dawood, Montather F. Ramadan, Zaid H. Mahmoud, Mohammed A. Farhan, Hasan Köten, Ehsan Kianfar

PII: S2666-0164(23)00131-7

DOI: <https://doi.org/10.1016/j.cscee.2023.100426>

Reference: CSCEE 100426

To appear in: *Case Studies in Chemical and Environmental Engineering*

Received Date: 4 May 2023

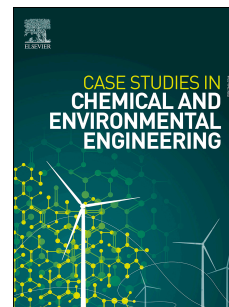
Revised Date: 12 July 2023

Accepted Date: 21 July 2023

Please cite this article as: H.N.K. AL-Salman, M.s. Falih, H.B. Deab, U.S. Altimari, H.G. Shakier, A.H. Dawood, M.F. Ramadan, Z.H. Mahmoud, M.A. Farhan, H. Köten, E. Kianfar, A study in analytical chemistry of adsorption of heavy metal ions using chitosan/graphene nanocomposites, *Case Studies in Chemical and Environmental Engineering* (2023), doi: <https://doi.org/10.1016/j.cscee.2023.100426>.

This is a PDF file of an article that has undergone enhancements after acceptance, such as the addition of a cover page and metadata, and formatting for readability, but it is not yet the definitive version of record. This version will undergo additional copyediting, typesetting and review before it is published in its final form, but we are providing this version to give early visibility of the article. Please note that, during the production process, errors may be discovered which could affect the content, and all legal disclaimers that apply to the journal pertain.

© 2023 Published by Elsevier Ltd.



A study in analytical chemistry of adsorption of heavy metal ions using chitosan/graphene nanocomposites

H. N. K. AL-Salman¹, Marwa sabbar Falih², Hiba B. Deab³, Usama S. Altimari⁴, Hussein Ghafel Shakier⁵, Ashour H. Dawood⁶, Montather F. Ramadan⁷, Zaid H. Mahmoud⁸, Mohammed A. Farhan⁹, Hasan Köten¹⁰, Ehsan Kianfar^{*10,11,12}

¹Department of pharmaceutical Chemistry, College of Pharmacy, University of Basrah, Iraq.

²Department of Chemistry, College of Science, Mustansiriyah University Baghdad, Iraq.

³University of Diyala, college of sciences, chemistry department of chemistry.

⁴Department of Medical Laboratories Technology, AL-Nisour University College/ Baghdad/ Iraq.

⁵College of pharmacy/ National University of Science and Technology, Dhi Qar, Iraq.

⁶department of medical engineering/ Al-Esraa University College, Baghdad, Iraq.

⁷college of Dentistry, Al-Ayen University, Thi-Qar, Iraq.

⁸University of Diyala, college of sciences, chemistry department of chemistry.

⁹University of Diyala, college of sciences, chemistry department of chemistry.

¹⁰Mechanical Engineering Department, Faculty of Engineering and Pure Sciences Istanbul Medeniyet University, Istanbul, Turkey.

¹¹Department of Chemical Engineering, Arak Branch, Islamic Azad University, Arak, Iran.

¹²Young Researchers and Elite Club, Gachsaran Branch, Islamic Azad University, Gachsaran, Iran.

* E-mail: ehsan_kianfar2010@yahoo.com and ehsankianfar775@gmail.com

Abstract

In this work, chitosan / graphene nanocomposite granules with weight percentages of 0.5%, 1%, 2% and 5% were prepared using a solution method. At first, graphene was oxidized with sulphuric and nitric acid then triethylenetetramine was grafted on graphene surface. Functionalized graphene was characterized by Fourier-transform infrared spectroscopy (FT-IR), Therapeutic Goods Administration (TGA), X-ray energy diffraction spectroscopy (EDX) and Scanning electron microscope (SEM). Results showed functionalization of graphene was successfully accomplished. The thermogravimetric analysis curves showed the pristine, oxidized and functionalized graphenes are stable up to 400, 250, and 300, respectively. The pristine graphenes are more stable than oxidized graphenes and the oxidized graphenes are more stable than functionalized graphenes. The observed stabilized temperature is known to be strongly influenced by the step of the functionalization. The morphology of nanocomposite was monitored by Scanning electron microscope (SEM). The SEM images showed that the porosity was reduced due to presence of nano graphenes. results showed that the nanocomposite samples have higher potential for ion metals adsorption than that of neat chitosan. The adsorption of nano samples for cadmium was increased around 20% in comparison to neat chitosan. Atomic adsorption spectrometry showed that the optimal adsorption rate of cadmium ion occurs in a solution of 50 ppm with a pH =7 and a contact time of 2 hours and an adsorbent of 25 mg.

Keywords: Adsorption, Heavy metal ions, Graphene nanocomposites, Chitosan, Polymer

1. Introduction

Water is a necessity required to sustain life. However, it is under serious threat because of the huge magnitude of pollution caused by industrial, agricultural, and domestic activities. Water bodies contaminated by heavy metals are grave problems because of their toxic nature and bioaccumulation [1-3]. Metal contamination may be due to domestic or industrial waste products, agricultural or municipal discharge, geologic weathering, and direct atmospheric

precipitation. These pollutants are often toxic. Long-term exposure to these pollutants can have acute and chronic effects on humans and animals [4-7]. Heavy metals, dyes, phenols, detergents, insecticides, and pesticides are some common pollutants. Owing to the ability of metals to remain in the environment for a long amount of time, they play a significant role in ecotoxicology. Bioaccumulation and biomagnification are common phenomena for heavy metals in the food chain. They are non-biodegradable in nature. Heavy metals at high concentrations exert significant environmental and ill effects on human health [8-11].

Chitin is an abundant natural polysaccharide and primarily isolated from crustacean biomass. It is a linear cationic heteropolymer containing N-acetyl-d-glucosamine units, some of which are linked to d-glucosamine units by β -(1-4) glycosidic bonds [12-15]. It exists as a matrix of proteins, minerals (calcium carbonate and phosphate), and lipids (unsaturated fatty acids [16-17]). Chitin is generally obtained from marine resources because of its commercial uses and is economical and abundant. Chitosan exhibits low solubility in neutral pH because of its inter- and intramolecular hydrogen bonds, its low antioxidant properties due to the lack of H atom donors, limited reactivity due to its high hydrophilicity, rigidity, and brittleness [18-21]. These properties have been studied and can be improved through modification through chemical, mechanical, or enzymatic methods [22-23]. Heavy metal ion removal from wastewater is always a difficult task for environmentalists. Chitosan is used efficiently for heavy metal removal because of its large surface area and high adsorption capacity, suitable pore size and volume, existence of large number of functional groups, mechanical stability, compatibility, easy accessibility, flexible structure of the polymer chain, high chemical reactivity, ease of regeneration, cost effectiveness, environmental friendliness, simple processing [24-26].

Isolated chitin is converted into chitosan by various enzymatic and chemical methods [27-29]. Various kinds of alkalis or acids are used in chitin deacetylation. Glycosidic bonds are susceptible to acids; hence, alkalis are considered appropriate options [30-32]. Chitin deacetylation can be achieved heterogeneously or homogeneously. Deacetylated chitin in a range of 85 %–99 % and can be used as an insoluble filtrate. It is processed using hot and concentrated NaOH solution. At 25 °C, chitin is dispersed in concentrated NaOH solution for 3 h and then suspended in crushed ice. The end product is soluble chitosan with a DA of approximately 48 %–55 % [33-35].

Chitin and chitosan and their derivatives due to their low cost and biodegradability as well as having a high amount of nitrogen and carboxylic carrier functional groups have attracted wide attention as an effective adsorption to remove various pollutants from water. These pollutants include metal cations and anions, radioactive materials, various pigments, phenols, as well as various anions and other pollutants [35-38]. Chitin and chitosan have a very high potential to remove such contaminants from water. However, there is still a need to find practical tools such as commercially developed surface adsorption [2,148-153]. For each adsorption process, having a large cross-sectional area, high pore volume and also having suitable functional groups are among the key and basic needs. To increase the adsorption rate of polymers, nanoparticles are used due to having the mentioned properties. Many nanoparticles, including Nano clays and carbon nanotubes, are currently being developed to remove contaminants from water. The nanoparticle that has recently attracted the attention of many scientists is called graphene. Graphene is a flat sheet with a thickness of 1 (one atom) composed of carbon atoms that are located in a crystal lattice of honeycombs. Graphene is the parent element of other carbon allotropes, including graphite, carbon nanotubes, and fullerene [39-41]. Among the unique

properties of graphene, we can mention its high mechanical, thermal and chemical flexibility. Graphene also has a very high specific cross-section, which makes it a potential candidate as high-performance adsorption. However, graphene in its original form does not have much ability to adsorption due to the lack of suitable functional groups. Because it has 2Sp atoms, it can only absorb pollutants with van der Waals forces [42-45]. The adsorption capacities of the above-mentioned chitosan -based adsorbents are summarized in Table 1.

Table1. The adsorption capacity of chitosan and its derivatives for other metal ions.

Adsorbent	Adsorbate	Adsorption Capacity	Reference
Glutaraldehyde crosslinked CS	Pd (II)	180.0 mg/g	[168]
Magnetic CS nanoparticles	Co (II)	27.5 mg/g	[168]
Magnetic crosslinked CS nanoparticles modified with ethylenediamine	Pt (IV)	171.0 mg/g	[169]
Magnetic crosslinked CS nanoparticles modified with ethylenediamine	Pd (II)	138.0 mg/g	[169]
MWCNT-PDA-CS-GO	Gd (III)	150.9 mg/g	[170]
CS-CE	Li (I)	297.0 mg/g	[171]

As well known that the abundant existence of toxic/heavy metal such as cadmium (Cd), chromium (Cr), Mercury (Hg) and lead (Pb) in environmental wastewater become serious problems and risks for human life. In general, they are issued during production processes of metal cleaning, plating dyes, leather industry. The privation of access to safe drinkable water has been widely reported with a lot of critical issues on human health problems. The presence of

these metals, even at extremely low concentrations, lead to occurrence of carcinogen in human as identified by the US National Toxicology Program. Thus, it is necessary to search some suitable direction for solving above problems. Several conventional technologies for removal of heavy metals are widely reported such as filtration membranes, ion-exchange, coagulation and co-precipitation processes. Unfortunately, these technologies cannot be well carried out under actual field trials since they present some disadvantages, for instance, the uses of expensive equipment and chemicals are required for wastewater treatment process [46]. The examples of CS derived adsorbents for Cd(II) have been summarized in Table 2.

Table 2. The adsorption capacity of CS and its derivatives for Cd (II).

Adsorbent	Adsorbate	Adsorption Capacity	Reference
ECH	Cd (II)	72.3 mg/g	[172]
CSAP	Cd (II)	84.0 mg/g	[173]
PMACCMs	Cd (II)	39.2 mg/g	[174]
Crosslinked	Cd (II)	178.6 mg/g	[175]
SMCS beads	Cd (II)	125.0 mg/g	[176]
Fe ₃ O ₄ loaded	Cd (II)	97.8 mg/g	[177]
CTS/SA/Ca ²⁺	Cd (II)	110.7 mg/g	[178]

In this study, chitosan / graphene-based nanocomposites were prepared with solution method and their ability to adsorb cadmium metal ions was investigated. The purpose of this article, investigate the adsorption of chitin and chitosan in the removal of heavy metal ions and also the obtained nanocomposite grains were obtained to obtain the optimal amount of adsorbent, pH, contact time and ion solution concentration was examined. Functionalized graphene was

characterized by Several characterization techniques (FT-IR, TGA, EDX and SEM) were also used.

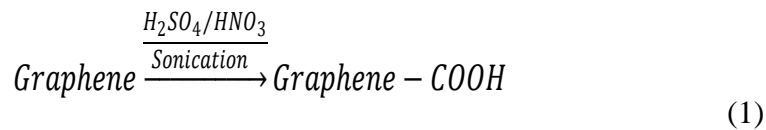
2. Materials and Experimental

2.1. Materials

All chemicals' materials (chitosan (75-75%), triethylene tetramine (97%), polyethylene glycol (30%), ethyl acetate (99%), sulfuric acid (99.9), nitric acid (65%), Formaldehyde (37%), Dimethylformamide (99%), Benzophenone (99%) were supplied from German company Merck and used without any future purification. All solution prepared by using distilled water[179].

2.2. Preparation of Graphene oxide

The purpose of graphene oxide is to place oxygenated functional groups such as carboxyl, carbonyl and hydroxyl groups on the surface of nanographene. To achieve this important and graphene oxide, a mixture of sulfuric acid and nitric acid was used. Initially, 0.3 g of graphene was placed in a vacuum oven for 24 hr at 80 ° C. The nanographene was then placed in 70 ml of M8 solution of 98% sulfuric acid and 65% nitric acid for oxidation and ultrasound for 37 kHz and w60 for oxidation [154-160]. The mixture was then removed from the ultrasonic bath and given 30 hours to reach room temperature. The mixture was then washed using a centrifuge to bring the pH of the mixture to about 4. Vacuum filtration was then used for washing due to reduced efficiency with the centrifuge[182-190]. The sample was washed with large amounts of double distilled water with a 0.45 μm polycarbonate filter to reach a pH of approximately 7. The sample was then placed in a vacuum at 80 ° C for 24 h to be completely dried. The above explanations are summarized in Equation 1[65-67].



Graphene has been synthesized from graphite by two fundamental processes, mechanical exfoliation and oxidation of graphite. However, the synthesis process has been categorized mainly into top-down and bottom-up approaches (Fig. 1)

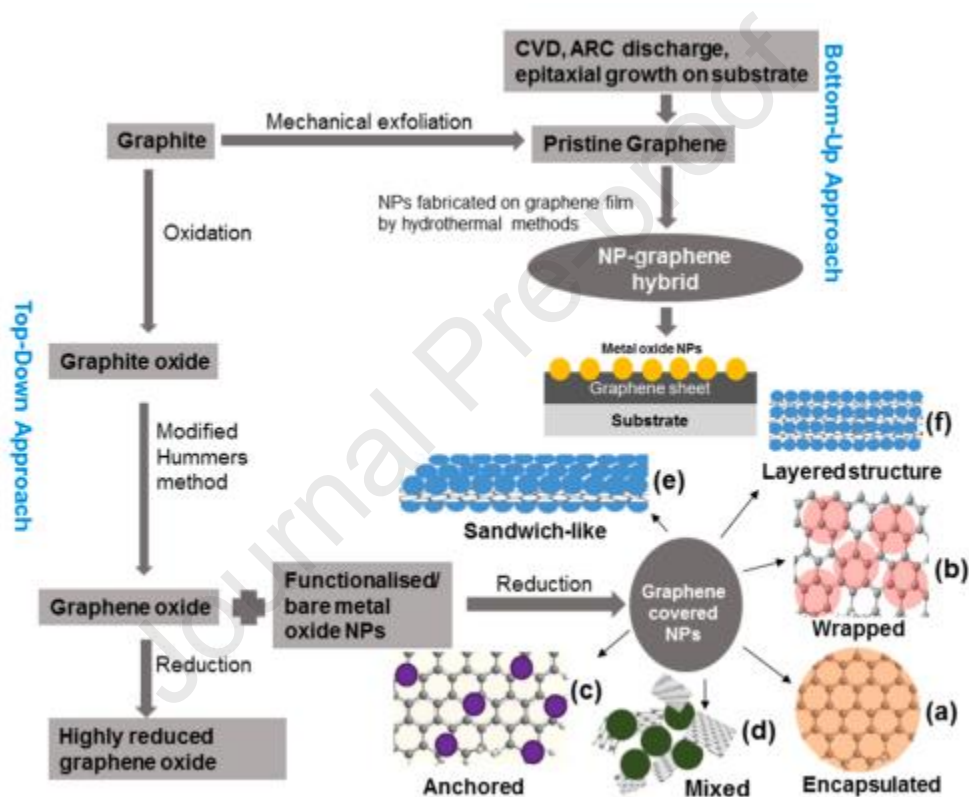


Fig1. Synthesis approach for graphene nanoparticles hybrids and their structures [180].

2.3. Preparation of Nano graphene acylation

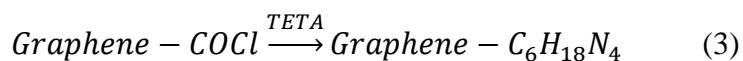
The acylation operation is used to deposit nitrogen functional groups on the surface of graphene after oxide because nitrogenous groups do not have the ability to react covalently with oxygenated functional groups. For this reason, acylation takes place so that chlorine reacts with oxygenated functional groups. After correction with acid and placement of oxygenated functional groups including carboxylic, hydroxyl and carbonyl on the surface of graphene, the acylation reaction was performed [161-164]. Thus, for 0.2 gr of oxidized graphene, 45 cc of thionyl chloride and 5 cc of dry dimethylformamide were used for the acylation reaction (ratio of dry thionyl chloride to dry dimethylformamide was 1:20). The time required for the acylation reaction was 120 min. The reflux reaction was performed at 60 °C and nitrogen atmosphere. The black precipitate was dried immediately after the reaction time with a sufficient amount of tetrahydrofuran and washed with a Teflon filter of 0.45 μ and placed in a vacuum at 8 ° C for 8 hr to dry completely. The process of the acylation process and the deposition of chlorine groups on the surface of oxidized graphene are shown in Equation 2[68-72]:



2.4. Preparation of nanographene

Triethylene tetramine was used to functionalize nanographene with nitrogen-containing groups. The reason for using this amine is its complete compatibility with water in all percentages and also having 4 nitrogenous functional groups in its chemical structure, which increases the adsorption of heavy metal ions. The functionalization was performed with adding 0.2 gr of this chlorinated graphene to 30 ml of triethylene tetramine and 3 ml of dry tetrahydrofuran after

acylation and drying of chlorinated graphene. The mixture is then subjected to 95 ° C for 24 hours to complete the functionalization operation. After 24 mixtures, the oil is taken out of the bath and given 30 minutes to reach room temperature. The mixture is then washed with a 0.45 µm Teflon filter with a mixture of water and ethanol one with one to remove excess unreacted amines from the system. It was then vacuumed for 40 ° C to dry completely. The reaction process of chlorine groups with triethylene tetramine is summarized in Equation 3[73-76]:



2.5. Preparation of Chitosan beads

First, 1 g of chitosan was poured into 50 ml of a 1% with volume solution of acetic acid and given 4 times for the chitosan to dissolve completely in the solution. Then 1 g of polyethylene glycol with a molecular mass of 200 gr / mol, which is in the form of resin, was added to it. Then, 2 ml of 37% with volume of aqueous formaldehyde solution was added to them and stirred for 2 minutes. The solution was then crosslinked and its viscosity was very high and poured into a 50 ml syringe. In parallel, 200 ml of 1 M sodium hydroxide solution was prepared and 1 ml of ethyl acetate was added and stirred vigorously for 20 were placed to mix thoroughly. Then, after preparing both samples, the cross-linked chitosan solution was poured dropwise into the sodium hydroxide solution to form chitosan granules. The sodium hydroxide solution was rested to harden. After that, the beads were washed 5 times with double distilled water so that no excess material was placed inside the beads [77-80].

2.6. Preparation of Chitosan grain nanocomposite

To prepare chitosan grain nanocomposites with wt0.5%, wt 1%, wt2%, and wt 5%, the following procedure was performed [81-83]:

A calculated amount of functionalized nano-phase was added to gr1 of the chitosan solution. The solution was then subjected to intense magnetic agitation for 3 days to disperse the nano-phase well into the polymer matrix. Then, as in the production of pure grain, polyethylene glycol and formaldehyde were added to make the grain nanocomposite cross-linked. The solution nanocomposite was then poured into a 50 ml syringe and, as before, dropwise was added to the caustic soda solution with ethyl acetate to form a granular nanocomposite.

2.7. Drying the beads

A dry cooling device was used to dry the grains. The grains were separated from the distilled water twice with filter paper and placed in a watch glass. The samples were then placed in a dry cooler for 48 hours to extract the water in the grains under vacuum and the samples were completely dry. After 48 beads were removed from the machine and placed in a sealed container with a dampener to be used in subsequent experiments [84-88].

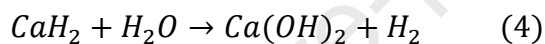
2.8. Method of making cadmium ion solution

A mother solution with a concentration of 1000 was used to make cadmium ion solution with different concentrations. To make the mother solution, the calculated amount of cadmium nitrate salt was dissolved in 1L of 0.5 M nitric acid solution [89-90].

2.9. Drying method of dimethyl formamide

Since the use of dry solvents is critical to the correction reaction, drying of dimethylformamide was on the agenda. The amount of 0.5-1 g of hydride, which is a solvent dehumidifier, is

weighed and ground; it was then poured into a 500 ml balloon and 400 ml of dimethylformamide was added. On the other hand, some cotton wool was placed in an increase-decrease interface and some calcium chloride was poured on it and it was covered with cotton again (as a protector). Calcium chloride absorbs moisture that is present in the air. This increasing-decreasing interface, called the drying tube, is placed on the balloon and then the mixture is stirred overnight with the help of a magnetic stirrer to mix calcium hydride well with the solvent and absorb the moisture in the solvent. This process is performed at room temperature and as a result of the reaction, hydrogen gas is produced which is removed from the system through the interface [91-95]. The reaction is as follows [96-98]:



After 24 h, the stirring was stopped and the balloon containing the solution was placed in an oil bath which was being heated. The distillation assembly was mounted on a balloon using a simple refrigerant and the temperature was raised to 130 ° C (dimethylformamide boiling temperature is 153 ° C). The system is connected to a vacuum to apply a vacuum to create suction and thus accelerate the movement of steam to the second balloon. Also creating a vacuum reduces the pressure and as a result the boiling point of dimethylformamide is lowered and the reaction is easier to achieve. On the other hand, the second balloon is placed inside the ice container to make the temperature difference easier for the condensed droplets to move into the balloon. The rotation of the magnetic agent also prevents the solvent from suddenly jumping into the balloon [99-101].

2.10. Drying method of tetrahydrofuran

Some sodium was added to 1 liter of tetrahydrofuran and poured into a balloon. Place the collector on the balloon and then the condenser on the collector while the collector valve is open. The balloon is heating and the THF is boiling [107-115]. The boiling point of tetrahydrofuran is 54.C. The resulting steam enters the collector from inside the balloon and then condenses. Condensation occurs in the condenser and returns to the balloon. The benzophenone reagent was added several times, indicating that the THF had dried each time it turned dark blue or blue. At this time, the collector valve is closed and THF vapors enter the condenser from the side pipe of the collector, condense and collect inside the collector [116-125]. Before collecting the dry THF in the container, about 300 gr of Molecular was placed in the oven at room temperature to activate. The activated molecular sieve was then placed in 250 ml jars and nitrogen gas was taken on it to evacuate the air inside the jar. The reason for using molecular sieve is that if THF gets dehydrated due to the impossibility of creating 100% isolation, these molecular sieves absorb moisture and prevent THF from getting wet. Then, with opening the collector outlet, the dried THF, which is ready for consumption, was poured into containers [126-130].

3. Results and Discussion

In this paper, first the results and discussions related to graphene functionalization reactions are presented and then chitosan beads and chitosan graphene nanocomposites are examined and their application in the adsorption of cadmium ions from aqueous solutions is investigated.

3.1. Determining the characteristics of functionalized graphene

3.1.1. Infrared Fourier Transform Spectroscopy (FTIR)

Observing the adsorption or transit peaks in the FTIR spectrum from the perspective of the presence or absence of operating groups helps to identify the substance. Of course, it should be

noted that accurate identification of the molecule or explicit detection of all peaks in a spectrum is not possible, and this analysis is used as a starting point in the identification process [136-138]. Figure 2 shows the FTIR spectrum of pure graphene, oxidized graphene, and graphene functionalized with triethylene tetramine (graphene containing nitrogen groups). As can be seen in Figure 1, the spectrum of pure graphene does not show an index peak and has many fine and crowded peaks due to the adsorption of moisture from the environment as well as impurities in graphene during production. In the acid-modified graphene spectrum, two index peaks are observed at 3424 and 1710, which are related to the vibration and tension of the OH groups and the C = O groups, respectively, due to the formation of hydroxyl and carboxyl groups in graphene, indicating that the oxide has been able to create oxygenated functional groups on the graphene plate [136-138]. After the acylation reaction and the placement of chlorine groups on the graphene plates, amine functional groups are immediately added to it and replace the chlorine groups formed on the graphene surface. As shown in Figure 2, two new peaks are observed in graphene functionalized with amine groups. The first peak is observed in 1572, which is related to the traction of N-H groups on the plate. There is also another peak in 800 which is related to the stretching of NH₂ functional groups off the screen [118]. Observing the peaks mentioned in Figure 2 proves the success of the oxide reaction and the functionalization of graphene with amine functional groups.

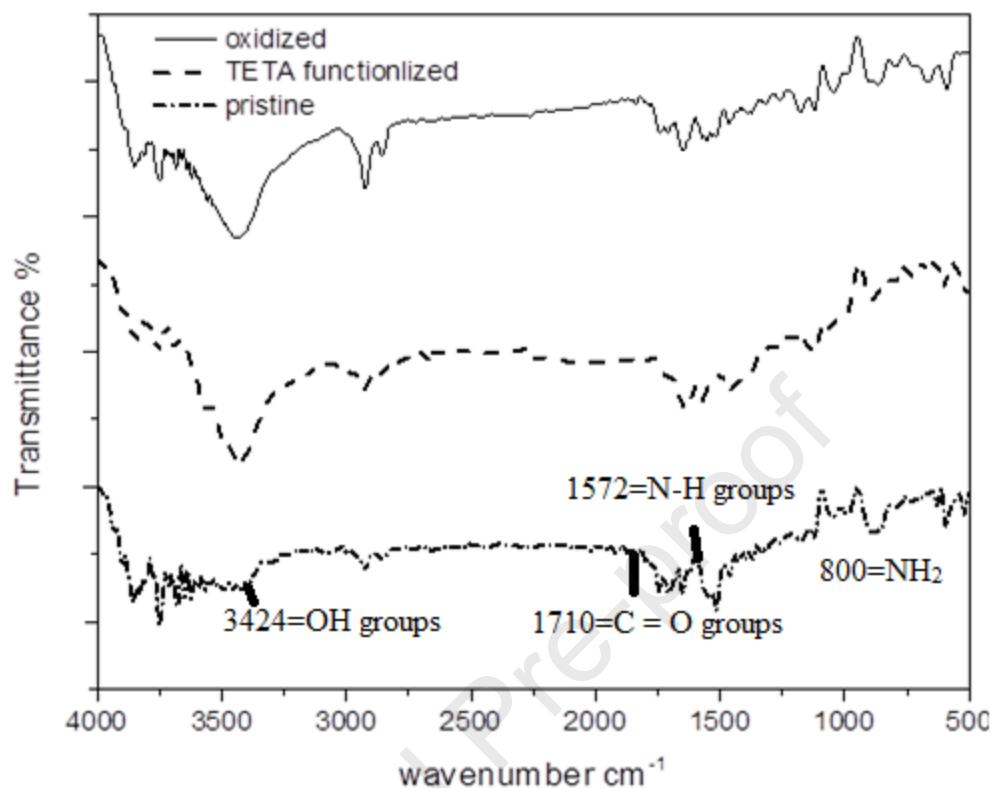


Figure 2. Infrared spectrum Fourier transform of samples.

3.1.2. Thermal gravimetric analysis (TGA)

Another method of evaluation to check and ensure the presence of functional groups on the graphene surface is thermal gravimetric analysis (TGA). The demographics of crude graphene, oxidized graphene, and triethylenetetramine-functionalized graphene are shown in Figure 3. As shown in Figure 3, weight loss occurs in both areas for all specimens. temperature range between 50 to 100 °C, which is due to physically absorbed moisture in the samples, this amount is the same for all samples. In the case of raw graphene, weight loss is observed in the temperature range between 150-800, which is related to graphene impurities during production. Next, with examining raw graphene and oxidized graphene, it is obvious that oxidized graphene

from about 150-800 has a more severe weight loss than raw graphene. The reason for this is the formation of oxygenated hydroxyl and carboxyl functional groups on the surface of graphene, which are continuously degraded with increasing the temperature to 800 and separated from the oxidized graphene surface, resulting in a heavier weight of oxidized graphene compared to raw graphene. Also, comparing functionalized graphene with crude graphene and oxidized graphene, it is obvious that triethylene-tetramine-activated graphene has a high degradation in the temperature range of 100-150, due to the degradation of triethylene tetramine taken on the surface of graphene.

Carbon-based adsorbents such as graphene and its derivatives, carbon nanotubes, activated carbon, and biochar are often used to remove heavy metals from aqueous solutions. One of the important aspects of effective carbon adsorbents for heavy metals is their tunable surface functional groups. To promote the applications of functionalized carbon adsorbents in heavy metal removal, a systematic documentation of their syntheses and interactions with metals in aqueous solution is crucial. This work provides a comprehensive review of recent research on various carbon adsorbents in terms of their surface functional groups and the associated removal behaviors and performances to heavy metals in aqueous solutions. The governing removal mechanisms of carbon adsorbents to aqueous heavy metals are first outlined with a special focus on the roles of surface functional groups. It then summarizes and categorizes various synthesis methods that are commonly used to introduce heteroatoms, primarily oxygen, nitrogen, and sulfur, onto carbon surfaces for enhanced surface functionalities and sorptive properties to heavy metals in aqueous solutions. After that, the effects of various functional groups on adsorption behaviors of heavy metals onto the functionalized carbon adsorbents are elucidated. The surface chemistry of carbons is determined, to a large extent, by the number and the nature of surface

functional groups on carbon surface [49], [130]. Several studies have provided evidences of the enhanced heavy metal adsorption capacity with modifications of carbon adsorbents with functional groups [53], [56], [131], [132], [133]. The driving mechanism of the modifications lies with the introduction of various functional groups into carbon materials through doping heteroatoms onto carbon. Carbonaceous materials including activated carbon (AC), biochar, carbon nanotubes (CNTs), and graphene oxide (GO) have been widely studied for adsorption of various environmental contaminants [20], [21], [22], [23], [24], [25], [26], [27], [28]. Their performance for the removal of heavy metals from aqueous solution has been widely reported [29], [30], [31], [32], [33], [34], [35], and most studies in the literature focus on sorption characteristics of a specific carbon material. AC is the most widely used carbon adsorbent for water and wastewater treatment. A wide range of AC adsorbents can be prepared to suit for various environmental applications including the removal of heavy metals from aqueous solutions [22], [36]. Due to the high cost associated with production of coal-based AC, biochar has recently emerged as a low-cost alternative of AC with comparable or superior performance for heavy metal adsorption [19], [37], [38], [39]. A variety of woody biomass including agricultural wastes or byproducts such as peanut hull and dairy manure can be used to develop biochar [40], [41], [42]. Its multifunctionalities including carbon sequestration, soil fertility improvement, and environmental remediation are also well recognized [25,43].

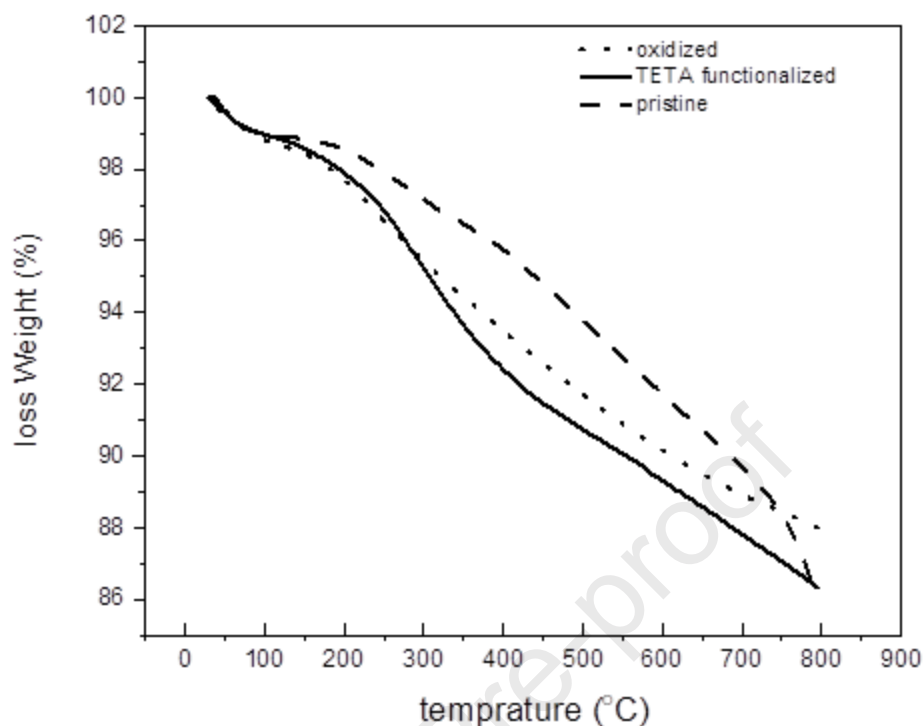


Figure 3. Demographics of pure, oxidized and functionalized graphene nanoparticles.

3.1.3. Morphology of nanoparticles using scanning electron microscope (SEM)

The SEM micrograph of the oxidized graphene and functionalized graphene is shown in Figure 4. As can be seen from Figure 4, raw graphene sheets have clustered together due to the absence of functional groups. With oxidizing graphene due to the formation of oxygenated groups on the surface, the graphene plates are completely separated from each other and become a single plate. Also, the sharp edges of oxidized graphene indicate the formation of oxygen groups on the surface of graphene. In the case of amine-functionalized graphene, however, the functionalized graphene plates are slightly rounded due to the reduction of oxygenated functional groups on the oxidized graphene surface and edge, and the deposition of nitrogen-functionalized functional groups on the graphene surface. Also, with examining scanning electron microscopy and

comparing the size of the plates in all three cases, it is observed that oxidation and functionalization of nanoparticles do not have much effect on the size of graphene plates. Another way to study and identify graphene oxide and functionalize it with amino groups is to use EDX elemental analysis (scanning electron microscope). In this analysis, the percentage of carbon, hydrogen, nitrogen and sulfur elements is determined. The test results are presented in Table 3. As can be seen, the amount of oxygen groups after correction with acid has increased significantly and from 5.7% to 14.22%. The presence of oxygen in unmodified graphene is related to the impurities present and the physically absorbed moisture of the environment. However, the increase in oxygen content in the modified graphene is related to the formation of oxygen-containing groups. In the case of functionalized graphene, while the amount of oxygen groups decreased from 14.22% in oxidized graphene to 7.05% in functionalized graphene due to graphene reduction, a large amount of nitrogen of about 32.67% sat on the graphene surface. This high amount of nitrogen is due to the type of amine consumed with triethylene tetramine, which has 4 amine groups and as a result contains a large percentage of functionalized nanographene. Figure 5 shows the distribution of oxygen and nitrogen elements as well as the amount of these elements in percentage.

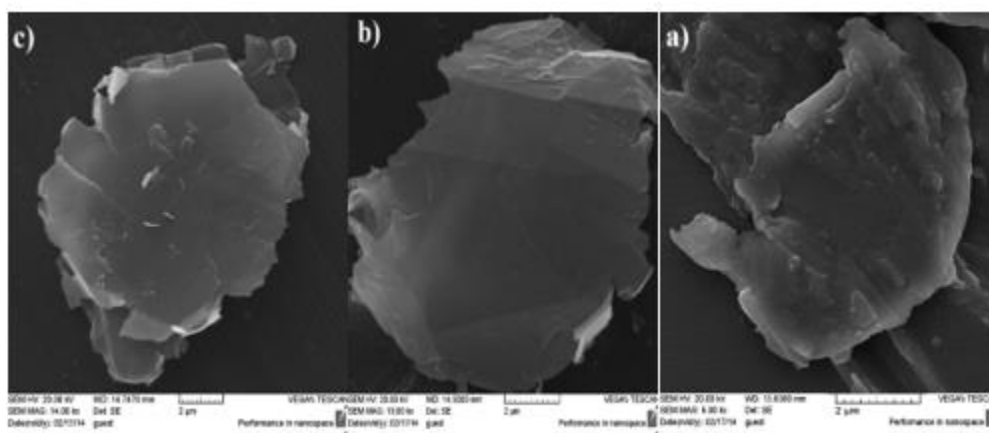


Figure 3. Scanning electron microscopy of (a) graphene nanoparticles and (b) oxidized graphene nanoparticles and (c) graphene nanoparticles functionalized with triethylene tetramine

Table 3. Elemental analysis data for samples.

Sample name	Carbon	Oxygen	Nitrogen	Other elements
Raw graphene	88	5.7	0	6.3
Oxidized graphene	80.78	14.22	0	5
Activated graphene	60.09	7.05	32.67	0.19

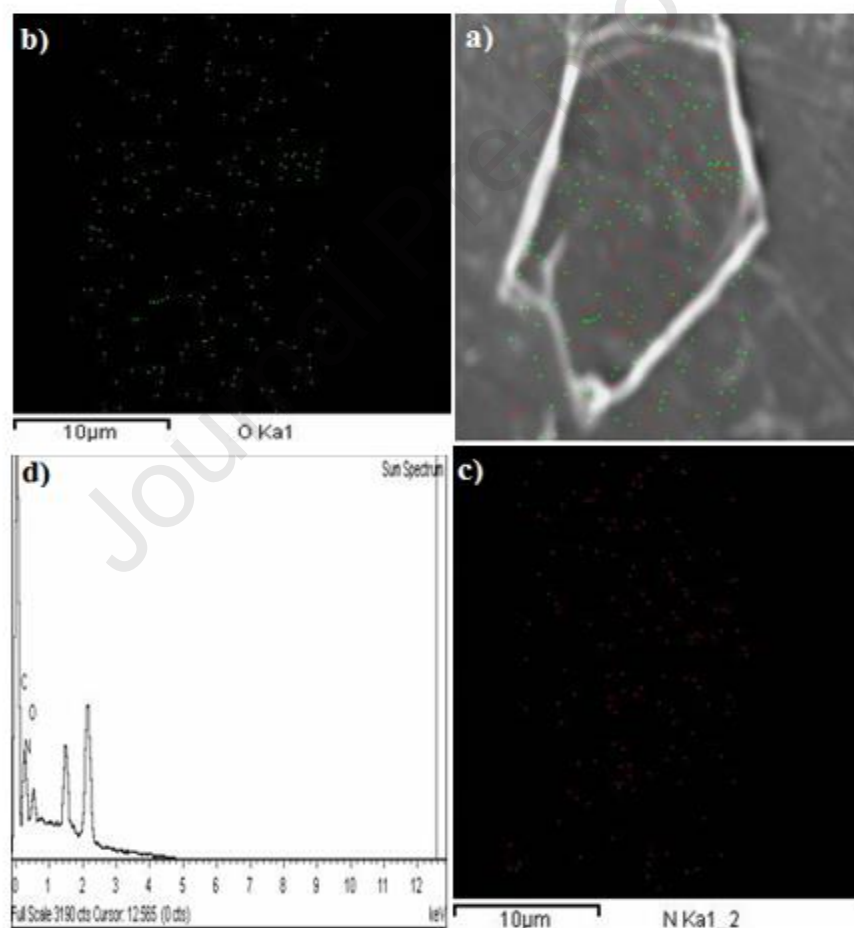
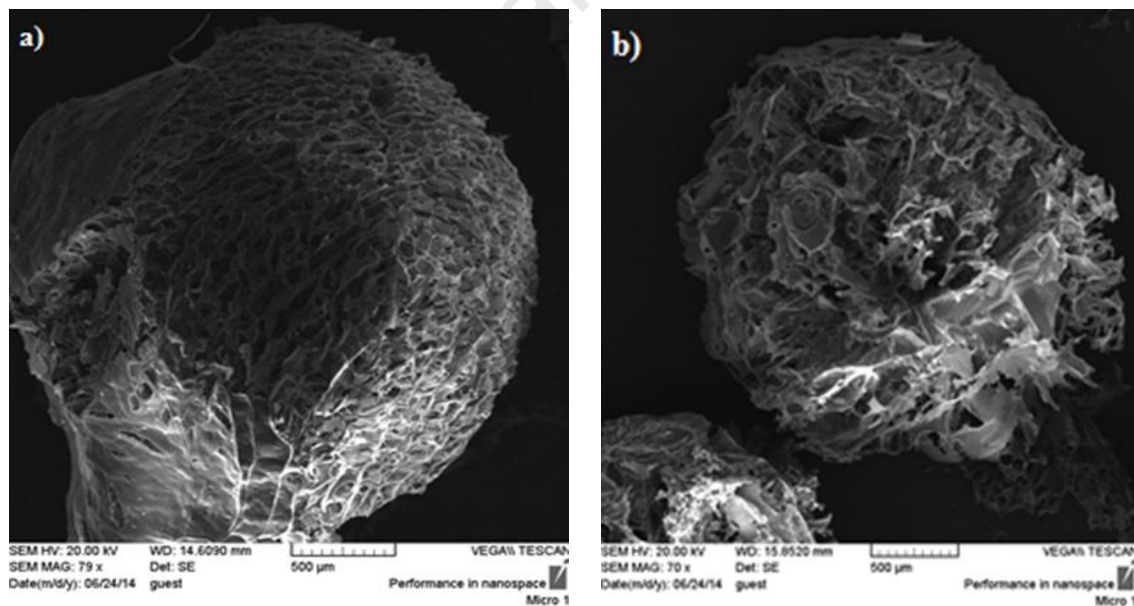


Figure 5. EDX images Scanning electron microscopy of a layer of graphene functionalized with triethylene tetramine (a distribution of oxygenated (green) and nitrogen-functional (red))

functional groups (b) distribution of oxygenated functional groups (c) distribution of nitrogen-functionalized groups) d Graph showing the percentage of carbon, oxygen and nitrogen groups

3.1.4. Investigation of porosity of nanocomposites

Since adsorption porosity has an important effect on the adsorption of heavy metal ions, scanning electron microscopy was used to study the grain porosity of nanocomposites and their porosity. As can be seen from scanning electron microscopy in figures 6 – 7 with different magnifications, the porosity of chitosan grains decreases with increasing percentage of functionalized graphene. This decrease in porosity increases with increasing weight percentage of nanoparticles because functionalized graphene nanoparticles are placed inside the pores of chitosan grains. Also, the porosity of chitosan grains is uniformly reduced, which indicates the complete dispersion of graphene nanoparticles within the polymer matrix.



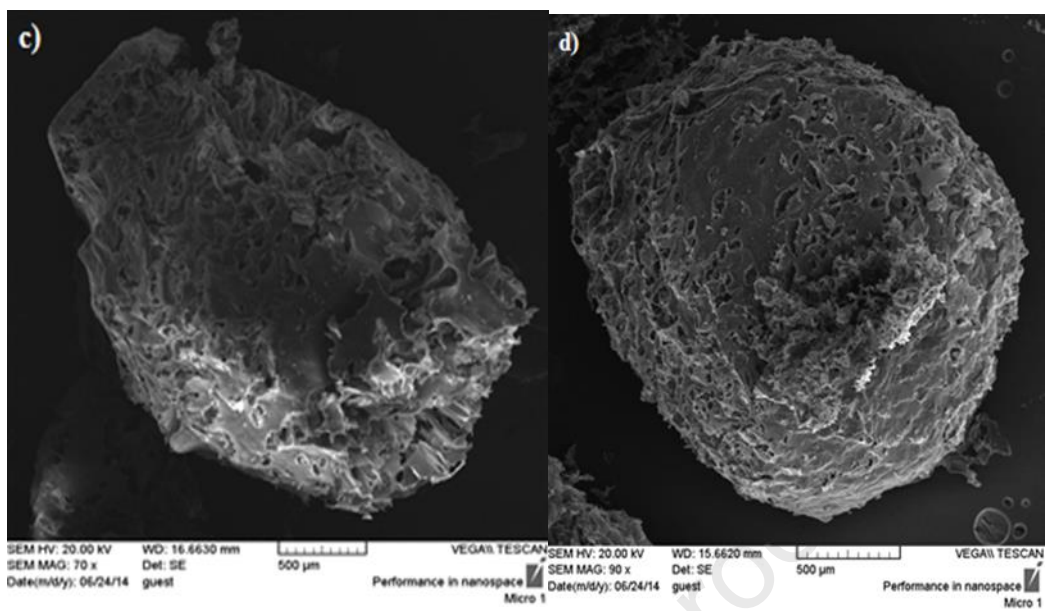
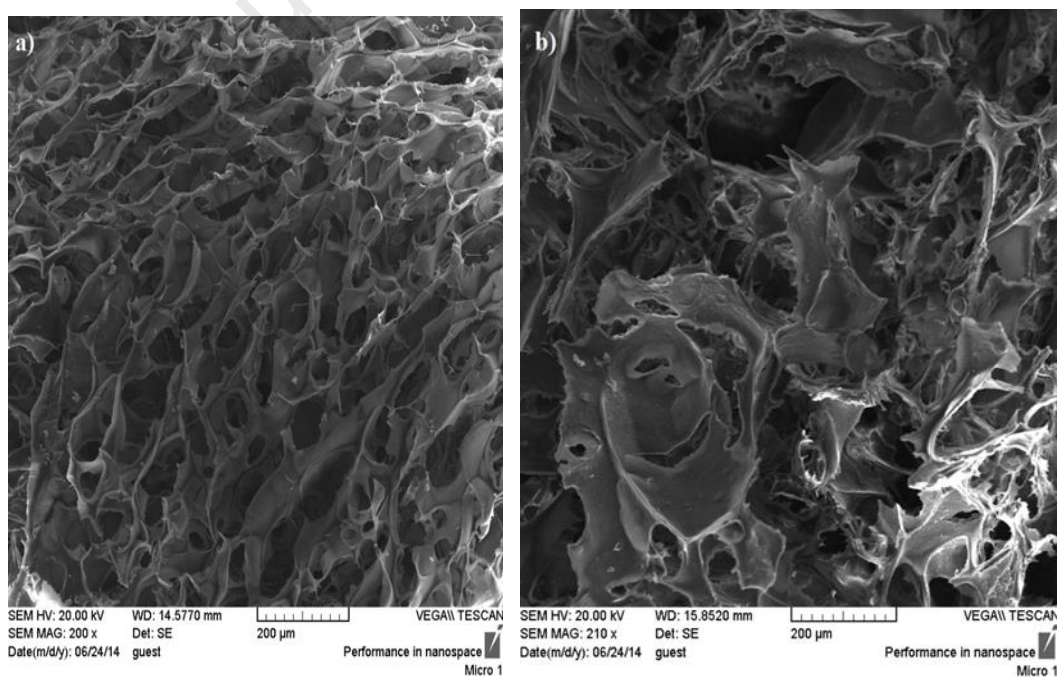


Figure 6. Scanning electron microscopy of chitosan grain with 70x magnification (a without functionalized graphene nanoparticles (b containing 1% with weight of functionalized graphene) c containing 2% with weight of functionalized graphene and (d containing 5% with weight of functionalized graphene has been hanged).



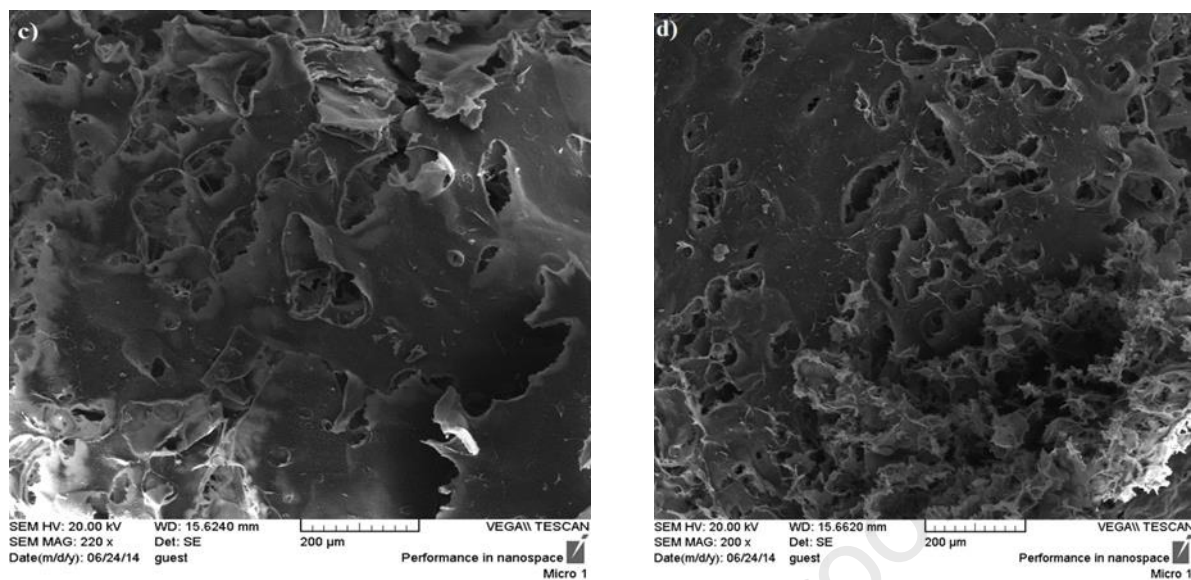


Figure 7. Scanning electron microscope of chitosan grain with 200x magnification (a without functionalized graphene nanoparticles) b) with 1% with weight of functionalized graphene (c with 2% weight of functionalized graphene and d) with 5% weight of functionalized graphene.

3.1.5. Investigation of the effect of swelling and water adsorption of chitosan nanocomposites

The porosity of chitosan grains as an adsorbent phase plays an important role in water uptake and thus uptake of heavy metal ions. The following method was used to evaluate the swelling and water adsorption of chitosan nanocomposites and compare it with pure chitosan granules.

0.1 g of the adsorbents was weighed dry with different percentages of functionalized graphene and then twice distilled into water at a pH of 6 and given 24 hours to complete the adsorption process with the adsorbents. The samples were then taken out of the water and weighed again after the excess water was removed with them. Then, through the Equation 5, the uptake and swelling of chitosan seeds were obtained:

$$\text{Percentage of swelling} = (W_s - W) / W \times 100 \quad (5)$$

Where it is equal to the weight of swollen grains in water in gr and W is equal to the weight of dry grains in gr.

The amount of swelling obtained from pure samples and nanocomposites with different percentages of functionalized graphene is presented in Table 4.

Table 4. Percentage of swelling of various adsorbents in double distilled water with pH 6

Adsorbent	Inflation rate
Pure chitosan seeds	49
0.5% Nanocomposite chitosan	37
1% chitosan nanocomposite	32
2% Nanocomposite chitosan	28
5% Nanocomposite chitosan	21

Kyzas et al[165] It is well known that chitosan-based materials serve as efficient adsorbents for dyes. This type of materials undergoes swelling with finite rate, when they are immersed in water, until to reach an equilibrium (steady state) volume. A problem that has been overlooked in the literature is the interaction between the two phenomena of swelling and adsorption. The characteristic times of two phenomena are comparable, so the swelling state of the adsorbent particle affects adsorption kinetics. In the present work, the interaction between these two phenomena is studied for several combinations of chitosan-based adsorbents and dyes, using experimental and theoretical tools. Several experiments for different polymeric adsorbents (chitosan derivatives) and dyes (reactive and basic) were performed. It is clearly shown that the adsorption kinetics are sensitive to the time of the adsorbent immersion in water. A unified

swelling-adsorption model is developed. This model is shown to be able to describe/reproduce the experimental data and allow their proper interpretation in terms of physicochemical processes. The interaction between adsorption dynamics and swelling dynamics in case of polymeric adsorbents based on chitosan and dyes as adsorbates is studied in the present work. An experimental campaign that includes three adsorbents and two dyes is performed. The adsorbent particles are immersed in water for several time periods before typical adsorption kinetic experiments to take place. It was found that the time of immersion (called pre-swelling time) has very large influence on the adsorption.

Liangzhi Qiao et al[166] Dye contamination of water supplies has a serious threat to human health, prompting the development of highly effective and eco-friendly adsorbents. In this work, polyelectrolyte microspheres derived from positively charged chitosan and negatively charged cellulose were constructed in alkali/urea solvent by a simple water/oil emulsification. The obtained chitosan/cellulose microspheres (CCM) were further used for the removal of reactive black 5. By using alkali/urea solution as the solvent, a homogeneous chitosan/cellulose solution was achieved, which avoided the easy occurrence of agglomeration between oppositely charged polymers. More importantly, CCM showed significantly improved mechanical strength and anti-swelling properties compared with pure chitosan microspheres (CM). Adsorption experiments demonstrated that CCM can effectively remove reactive black 5 with high adsorption capacity of 214.36 mg/g, fast adsorption kinetic that reached 76% of the equilibrium adsorption amount within only 20 min, and good reusability that maintained 75% efficiency even after five times of adsorption/desorption cycle, indicating a great potential for the application of dye removal.

3.1.6. Adsorption of cadmium ion from aqueous solutions with nanocomposite of functionalized chitosan graphene hydrogels

In order to investigate the adsorption of cadmium ion from aqueous solutions, experiments were performed in 4 different groups in a row to obtain the optimal adsorption rate and compare it with the adsorption rate with raw grain. These 4 groups are as follows:

- ✓ Obtaining the optimal adsorber.
- ✓ Determining the optimal pH.
- ✓ Obtaining the optimal call time.
- ✓ Obtaining the optimal concentration of cadmium ion.

3.1.6.1. Obtaining the optimal amount of adsorbent cadmium ions

In order to obtain the optimal amount of adsorbent, 15mg, 20mg, 25mg and 30mg of adsorbent were added to 10ml of cadmium ion solution with a concentration of 50ppm, respectively, and the pH of the solution was reduced to 5 with 0.1 M NaOH solution. The samples were then placed on a vibrating stirrer at 200rpm. After one hour, the samples were separated from the ionic solution with means of a filter and atomic adsorption test was taken from the ionic solutions. The amount of cadmium ion in each of the solutions was obtained using an atomic adsorption spectrometer and then the amount of divalent cadmium ion adsorption in terms of mg based on 1gr of the adsorbent was obtained using Equation 6:

$$\text{Adsorption capacity}(q_e) = \frac{(C_0 - C_e)V}{M} \quad (6)$$

In this equation, it is equal to the concentration of the initial ionic solution in terms of ppm before the adsorption process and is equal to the concentration of the ionic solution in terms of

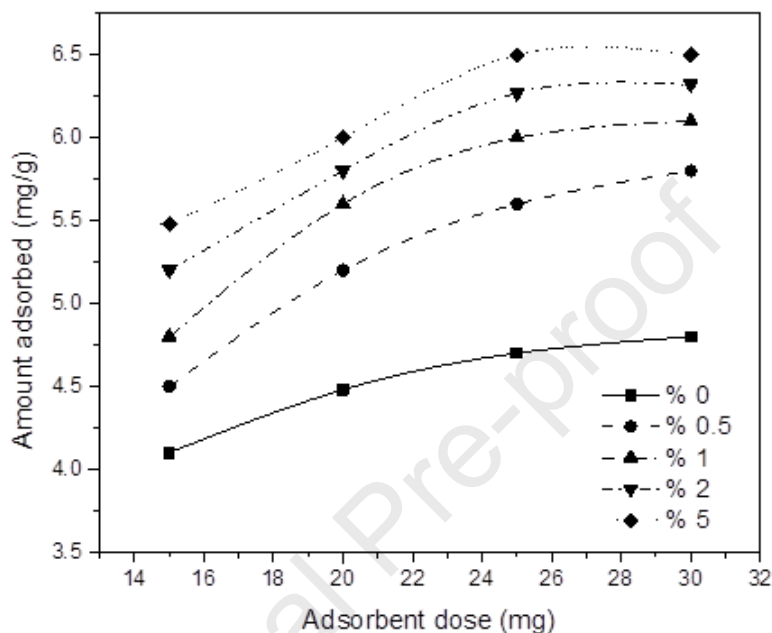
ppm after the adsorption process. Also, V is equal to the volume of ionic solution of each sample in ml and W is equal to the amount of adsorbent used in terms of gr in each sample. It is also equal to the adsorption of cadmium ions in mg in terms of 1 g of adsorbent (chitosan and chitosan nanocomposite).

As can be seen from Figure 8, the rate of uptake of cadmium ion with pure chitosan grains is between 4-5 mg of cadmium ion per gram of adsorbent due to the different amount of adsorbent. However, with adding different percentages of functionalized graphene to chitosan seeds, the amount of adsorption increases significantly. The reason for the increase in adsorption is that graphene nanoparticles functionalized with triethylene tetramine have a large number of active amine sites on their surface. With increasing these nanoparticles to chitosan beads, cadmium metal ions are more adsorbed to these active sites. So, the adsorption rate increases. It is also noteworthy from the figure that with increasing the amount of adsorbent up to 25mg, the amount of adsorption increases with a large slope and then the slope of increasing the amount of adsorption decreases. Therefore, the optimal amount of adsorbent is equal to 25 mg and other tests will be performed with the same amount of adsorbent. Another noteworthy point is that with increasing the percentage of functionalized graphene to chitosan grains, the amount of adsorption increases; but the adsorption rate is not very significant. The reason for this is that with increasing the percentage of functionalized nanographene to chitosan beads, the porosity and water adsorption of these beads decreases. Therefore, the penetration of cadmium metal ions into chitosan beads is reduced. For this reason, even with a significant increase in the active sites of amines, the adsorption of cadmium metal ions increases significantly. Reduction of chitosan grain porosity can be demonstrated with scanning electron microscopy photographs as well as water uptake test and investigation of increased swelling behavior of chitosan grains in water.

Preeti Pal, Anjali Pal [139] the present study explores a new SDS-modified chitosan-based material for Cd^{2+} removal from aqueous media. The modified beads are designated as SMCS beads. During modification of chitosan (CS) beads, the SDS concentration is selected as CMC which leads to the formation of a surfactant bilayer on the chitosan beads. Cd^{2+} ions can be adsorbed on the surfactant bilayer by electrostatic attraction. This causes much enhanced adsorption of Cd^{2+} compared to normal CS beads. Batch experiments have been carried out to optimize the process parameters such as pH, adsorbent dose, and SDS concentration (during modification of beads). The kinetics of the Cd^{2+} removal on SMCS beads indicates that, the adsorption follows pseudo-second order model. The equilibrium data fitted well to the Langmuir isotherm. The maximum adsorption capacity was found to be 125 mg/g. Time taken to attain equilibrium was 10 h which was expected due to the slow kinetics usually observed on CS beads. The ability of chitosan to adsorb heavy metals makes it an economically cheap and environmentally friendly adsorbent.

Alyasi et al [140] Industrial effluents and stormwater runoff pose a significant threat to the environment and public health. Consequently, the water quality guidelines set strict limitations on the heavy metal content due to their toxicity. Among heavy metals, cadmium is one of the most hazardous, and its maximum permissible concentration is 10 $\mu\text{g/L}$. Therefore, the improvement of wastewater treatment technology is a prominent and ongoing task. The present study deals with the adsorption of cadmium onto chitosan beads and nanochitosan, a natural polysaccharide polymer derived from seafood shell waste. The chitosan beads and the nanochitosan were derived from the same source chitosan in order to compare their capacities and their kinetic performances on an equal basis. Both cadmium adsorption capacities are extremely high with 1.65 mmol Cd/g chitosan beads and 1.90 mmol Cd/g on nanochitosan—with

nanochitosan showing a 15% higher uptake. Several kinetic models were compared and the kinetics of both chitosan beads and nanochitosan followed both the pseudo-second-order and the Elovich models very closely but the uptake of cadmium on nanochitosan was faster.



. Figure 8. Changes in the adsorption rate of cadmium ion in the presence of different percentages of functionalized nanoparticles and obtaining the optimal amount of adsorbent at pH =5 and duration 1h and concentration 50ppm.

3.1.6.2. Obtaining the optimal pH in the adsorption of cadmium ions

Considering that the optimal amount of adsorbent for adsorption of cadmium metal ion was equal to 25 mg, therefore 25 mg of adsorbents with different percentages of functionalized graphene was added to 10 ml of cadmium ion solution with a concentration of 50 ppm. To raise the pH of the ionic solution (since cadmium salt is dissolved in 0.5 M nitric acid and its pH is about 2.5) 0.1 M NaOH solution was added to the ionic solution with titration and the pH of the solution using a pH device M was determined. The samples were then placed on a vibrating

stirrer at 200 rpm for one hour to complete the adsorption reaction. The amount of cadmium ion remaining in the ionic solution was then determined by atomic adsorption spectrometry and the adsorption rate of each of the adsorbents at different pHs was obtained using the equation. As shown in Figure 9, at pH= 3, where the pH is completely acidic, the adsorption of cadmium ions in all samples is approximately equal, and this adsorption is equal to the minimum adsorption at all pHs. The mechanism of cadmium ion adsorption is such that the active sites of amines in adsorbents have a negative charge. Adsorption of positively charged divalent cadmium ions occurs through electrostatic interaction and chelating process with negatively charged active sites in the adsorption phase. Chelation is the process with which a chemical compound combines with a metal ion to hold it in place. Materials with such properties are used to adsorb heavy metal ions. It should be noted that chelating refers to a ligand that gives more complex electrons to the central metal of the complex. Therefore, as the number of negatively charged active sites increases, the amount of cadmium ion uptake increases. At acidic pHs the number in solution is extremely high. Thus, a competition is made to react with the active sites of amines between and. Due to the high rate, these active sites establish an electrostatic interaction, and the negative amine active sites are reduced. As a result, their ability to form complexes with cadmium metal ions is lost. Therefore, the adsorption of cadmium ions is reduced. As the pH rises, the amount in solution decreases. As a result, the active sites of the amine react more strongly with the metal cadmium ions. So, the adsorption of cadmium ions increases. This increase in adsorption rate continues until pH= 7, and as shown in the figure, then the adsorption rate decreases slightly. The reason for decreasing the amount of adsorption with increasing is that with increasing the pH, the amount in solution increases. The ion solution in the positively charged cadmium ion establishes an electrostatic interaction, as a result of which the ability to establish an electrostatic

interaction and the cadmium ion chelation process with the negatively charged amine active sites is lost. Therefore, cadmium precipitates as salt. Therefore, the adsorption of cadmium ions decreases. Due to the fact that the highest amount of adsorption occurred in all samples at pH =7, in other experiments the pH of solutions is considered equal to.

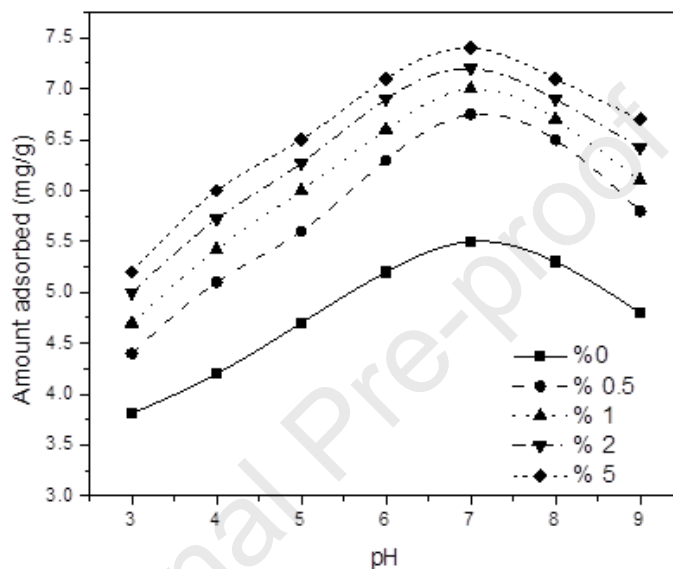


Figure9. Graph of changes in the adsorption rate of cadmium ion with adsorbents with different percentages of graphene functionalized at different pHs with an adsorbent of 25 mg and a duration of 1 h and a concentration of 50 ppm

3.1.6.3. Obtaining the optimal contact time to adsorbent cadmium ions

25mg of adsorbents with different percentages of functionalized graphene was added to 10 ml of cadmium ion solution with a concentration of 50 ppm and a pH = 7. The samples were then placed on a vibrating stirrer at 200 rpm. In order to obtain the optimal contact time, the experiments were performed in time intervals of 30min, 60min, 120min and 240 min. As shown in Figure 10, the adsorption rate of cadmium ions generally increases with increasing contact time between the adsorbent phase and the cadmium metal ions. But this increase increases after

120min to 240min with a much smaller slope. Because according to the results obtained after 120 min, almost all active amine sites have been able to interact electrostatically with cadmium metal ions and only a few of them are still active and for a longer time to Need to perform the adsorption process. Therefore, due to the fact that the adsorption rate is almost complete after 120 min, the optimal contact time of 120 min was considered in other experiments.

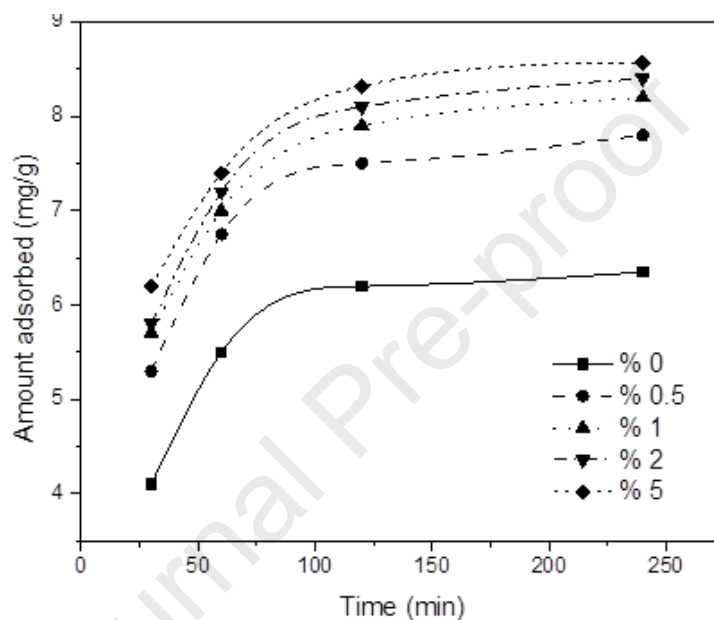


Figure 10. Changes in the amount of cadmium ion adsorption with adsorbents with different percentages of functionalized graphene at different times at pH = 7 and the amount of adsorbent 25mg and concentration 50ppm.

3.1.6.4. Obtaining the concentration of cadmium ion for optimal adsorption of cadmium ion

25mg of the adsorbent phase with different percentages of functionalized graphene was placed in 10 ml of cadmium ion solution with a pH =7. Cadmium ion concentrations in each sample

were considered equal to 20ppm, 30ppm, 50ppm and 100ppm, respectively. The samples were then placed on a vibrating stirrer at a speed of 200 rpm and given 120 minutes to complete the adsorption process. As shown in Figure 11, the adsorption rate increases with increasing cadmium ion concentration. This is because with increasing the concentration of cadmium ions, the active sites of amines, which are not able to contact cadmium ions well, are exposed to more metal ions with increasing the concentration of cadmium ions, and as a result, the adsorbent capacity is significantly higher.

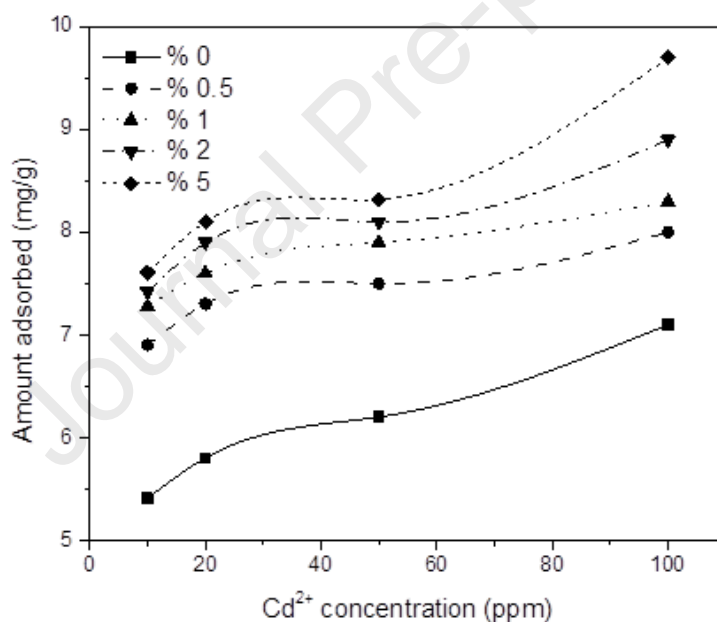


Figure 11. Changes in the rate of adsorption of cadmium ions with adsorbents with different percentages of graphene functionalized at different concentrations of cadmium ions and durations of 2 h at pH = 7 and the amount of adsorbent 25mg.

5. Future prospective and sustainability of magnetic graphene materials

The water chemistry makes the remediation process quite complicated, as contaminants may form new toxic compounds and cause environmental hazards because of anonymous interactions, fate and mobility in the aqueous solution [140-145]. Fig. 12 illustrates the application of magnetic graphene functionalized composites for different contaminants either using ion exchange, reduction, oxidation, precipitation, hydrolysis, etc. which commonly highlights the adsorption method as a significant procedure for wastewater treatment [181]. Magnetic graphene-based chemically functionalized composites are projected to remediate heavy metals. However, the research on remediation of combined contaminants using magnetic graphene-based composites or nanomaterials is still under progress. Though novel magnetic graphene-based functionalized composites have significant potential to remediate contaminants with enhanced adsorption capacity and for environmental application, e.g., fate, mobility, ecotoxicity, and risk assessment of contaminants. Adsorption capacity and toxicity of contaminants strongly depend upon aqueous solution chemistry as well as physicochemical characteristics, such as particles sizes, functional groups, potential surface charges and specific surface area.

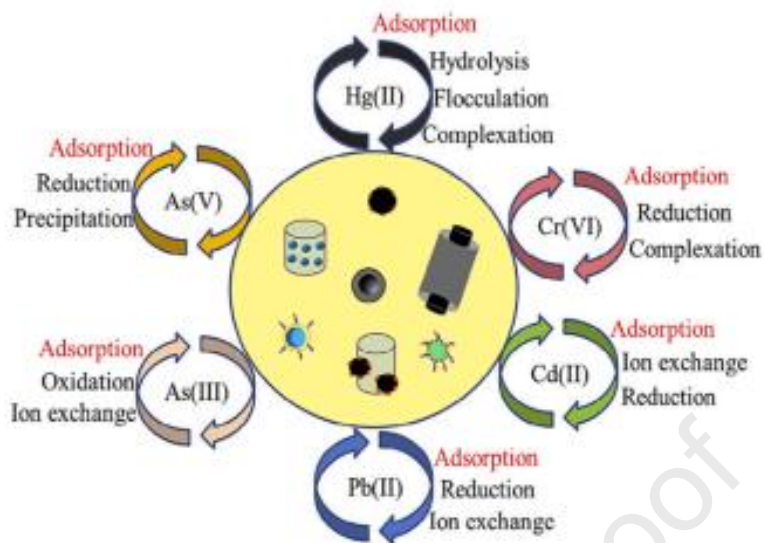


Fig. 12. Highlighting the application of different wastewater treatment methods, including adsorption for heavy metals removal using different magnetic graphene functionalized composites [181].

6. Conclusions

In this study, chitosan / graphene-based nanocomposites were prepared with solution method and their ability to adsorb cadmium metal ions was investigated. The following results can be obtained from this study:

- Oxygenated functional groups on graphene surface were induced by acid test and identified with FTIR, EDX and TGA tests and their accuracy was confirmed.

Triethylene tetramine was grafted on the surface of oxidized graphene and this grafting was confirmed with FTIR, EDX, TGA tests.

Chitosan granules and chitosan / graphene functionalized nanocomposites were prepared and the swelling and adsorption of cadmium metal ions with these adsorbents were investigated.

SEM micrographs showed the effect of functionalized graphene on chitosan grains and the porosity of these grains with reducing the porosity of the samples.

- The obtained nanocomposite grains were obtained to obtain the optimal amount of adsorbent, the optimal amount of pH, the optimal amount of contact time and the optimal amount of ion solution concentration with these adsorbents in cadmium ion adsorption and the results of significant improvement in cadmium ion adsorption.

Declarations

Ethical Approval

Not applicable

Competing interests

The author declare that they have no competing interests.

Authors' contributions

H. N. K. AL-Salman, Marwa sabbar Falih, Hiba B. Deab, Usama S. Altimari, Hussein Ghafel

Shakier: reviewing and editing.

Ashour H. Dawood, Montather F. Ramadan, Zaid H. Mahmoud, Mohammed A. Farhan:

reviewing and editing.

Hasan Köten, Ehsan Kianfar : Investigation, writing – original draft, reviewing and editing.

Funding

Not applicable

Availability of data and materials

Not applicable

Reference

- [1]. Begum, S., Yuhana, N. Y., Saleh, N. M., Kamarudin, N. H. N., & Sulong, A. B. (2021). Review of chitosan composite as a heavy metal adsorbent: Material preparation and properties. *Carbohydrate polymers*, 259, 117613.
- [2]. Haripriyan, U., Gopinath, K. P., & Arun, J. (2022). Chitosan based nano adsorbents and its types for heavy metal removal: A mini review. *Materials Letters*, 131670.
- [3]. Philibert, T., Lee, B. H., & Fabien, N. (2017). Current status and new perspectives on chitin and chitosan as functional biopolymers. *Applied Biochemistry and Biotechnology*, 181(4), 1314–1337. <https://doi.org/10.1007/s12010-016-2286-2>.
- [4]. Hajji, S., Younes, I., Ghorbel-Bellaaj, O., Hajji, R., Rinaudo, M., Nasri, M., et al. (2014). Structural differences between chitin and chitosan extracted from three different marine sources. *International Journal of Biological Macromolecules*, 65, 298–306. <https://doi.org/10.1016/j.ijbiomac.2014.01.045>.
- [5]. Yadav, M., Goswami, P., Paritosh, K., Kumar, M., Pareek, N., & Vivekanand, V. (2019). Seafood waste: A source for preparation of commercially employable chitin/chitosan materials. *Bioresources and Bioprocessing*, 6(1). <https://doi.org/10.1186/s40643-019>.
- [6]Crini G., “Recent developments in polysaccharide-based materials used as adsorbents in wastewater treatment,” *Prog. Polym. Sci.*, 1, 38–70, Jan. 2005.
- [7]Benguella B., “Cadmium removal from aqueous solutions by chitin: kinetic and equilibrium studies,” *Water Res.*, 10, 2463–2474, May 2002.
- [8]Benguella B., Benaissa H., “Effects of competing cations on cadmium biosorption by chitin,” 143–150, 2002.

[9] Environ J., “Adsorption experiments, whereas a particle size of 328 μm was used for column studies. Determination of pH zpc A procedure outlined by Huang and Ostovic (1978) was used to determine the pH of the zero point of charge (pH zpc) of chitosan. To each o,” 4, 962–974, 1989.

[10] Sillanpää M. E., Rämö J. H., “Decomposition of beta-alaninediacetic acid and diethylenetriamine-pentaacetic acid by hydrogen peroxide in alkaline conditions,” Environ. Sci. Technol., 7, 1379–84, Apr. 2001.

[11] McKay G, Blair HS F. A., “Equilibrium studies for the sorption of metal ions onto chitosan,” Indian J. Chem., 356–360, 1989.

[12] Svetlana Verbycha, Mykhaylo Bryka G. C. & B. F., “Removal of copper (II) from aqueous solutions by chitosan adsorption,” Sep. Sci. Technol., 8, 1749–1759, 2005.

[13] McAfee B. J., Gould W. D., Nadeau J. C., Costa A. C. A., “BIOSORPTION OF METAL IONS USING CHITOSAN, CHITIN, AND BIOMASS OF RHIZOPUS ORYZAE,” Sep. Sci. Technol., 14, 3207–3222, Nov. 2001.

[14] BASSI R., PRASHER S. O., SIMPSON B. K., “Removal of Selected Metal Ions from Aqueous Solutions Using Chitosan Flakes,” Sep. Sci. Technol., 4, 547–560, Jan. 2000.

[15] Jeon C., Höll W. H., “Chemical modification of chitosan and equilibrium study for mercury ion removal,” Water Res., 19, 4770–80, Nov. 2003.

[16] Department G. L. R. and T.-Y. H. J. D. W., “Synthesis of Porous-Magnetic Chitosan Beads for Removal of Cadmium Ions from Waste Water,” Indian Eng. Chem. Res., 9, 2170–2178, 1993.

- [17]Liu X., Hu Q., Fang Z., Zhang X., Zhang B., “Magnetic chitosan nanocomposites: a useful recyclable tool for heavy metal ion removal.,” *Langmuir*, 1, 3–8, Jan. 2009.
- [18]Septum C., Rattanaphani S., Bremner J. B., Rattanaphani V., “An adsorption study of Al(III) ions onto chitosan.,” *J. Hazard. Mater.*, 1–2, 185–91, Sep. 2007.
- [19]Schmuhl R., Krieg H. M., Keizer K., “Adsorption of Cu (II) and Cr (VI) ions by chitosan : Kinetics and equilibrium studies,” *Water SA*, 1, 1–7, 2001.
- [20]Chen Y., Chen L., Bai H., Li L., “Graphene oxide–chitosan composite hydrogels as broad-spectrum adsorbents for water purification,” *J. Mater. Chem. A*, 6, 1992, 2013.
- [21]Chandra V., Park J., Chun Y., Lee J. W., Hwang I., Kim K. S., “Water-dispersible magnetite-reduced graphene oxide composites for arsenic removal.,” *ACS Nano*, 7, 3979–86, Jul. 2010.
- [22]Chandra V., Kim K. S., “Highly selective adsorption of Hg²⁺ by a polypyrrole-reduced graphene oxide composite.,” *Chem. Commun. (Camb)*, 13, 3942–4, Apr. 2011.
- [23]Zhang N., Qiu H., Si Y., Wang W., Gao J., “Fabrication of highly porous biodegradable monoliths strengthened by graphene oxide and their adsorption of metal ions,” *Carbon N. Y.*, 3, 827–837, Mar. 2011.
- [24]Li L., Fan L., Sun M., Qiu H., Li X., Duan H., Luo C., “Adsorbent for chromium removal based on graphene oxide functionalized with magnetic cyclodextrin-chitosan.,” *Colloids Surf. B. Biointerfaces*, 76–83, Jul. 2013.
- [25]Vasudevan S., Lakshmi J., “The adsorption of phosphate by graphene from aqueous solution,” *RSC Adv.*, 12, 5234, 2012.

- [26]Knaebel K. S., “ADSORBENT SELECTION”.
- [27]Wang Y., Chen X., Zhong Y., Zhu F., Loh K. P., “Large area, continuous, few-layered graphene as anodes in organic photovoltaic devices,” *Appl. Phys. Lett.*, 6, 063302, 2009.
- [28]Wang X., You H., Liu F., Li M., Wan L., Li S., Li Q., Xu Y., Tian R., Yu Z., Xiang D., Cheng J., “Large-Scale Synthesis of Few-Layered Graphene using CVD,” *Chem. Vap. Depos.*, 1–3, 53–56, Mar. 2009.
- [29]Seung B., Chae J., Gu F., Kim K. K., Kim E. S., Han H., Kim S. M., Shin H., Yoon S., Choi J., Park M. H., Yang C. W., Pribat D., Lee Y. H., “Synthesis of Large-Area Graphene Layers on Poly-Nickel Substrate by Chemical Vapor Deposition : Wrinkle Formation,” 2328–2333, 2009.
- [30]Li X., Cai W., An J., Kim S., Nah J., Yang D., Piner R., Velamakanni A., Jung I., Tutuc E., Banerjee S. K., Colombo L., Ruoff R. S., “Large-area synthesis of high-quality and uniform graphene films on copper foils.,” *Science*, 5932, 1312–4, Jun. 2009.
- [31]Di B. C., Wei D., Yu G., Liu Y., Guo Y., Zhu D., “Patterned Graphene as Source / Drain Electrodes for Bottom-Contact Organic Field-Effect Transistors **,” 3289–3293, 2008.
- [32]Dervishi E., Li Z., Watanabe F., Biswas A., Xu Y., Biris A. R., Biris A. S., “Large-scale graphene production by RF-cCVD method w,” 4061–4063, 2009.
- [33]Li N., Wang Z., Zhao K., Shi Z., Gu Z., Xu S., “Large scale synthesis of N-doped multi-layered graphene sheets by simple arc-discharge method,” *Carbon N. Y.*, 1, 255–259, Jan. 2010.
- [34]Seyller T., Bostwick A., Emtsev K. V., Horn K., Ley L., McChesney J. L., Ohta T., Riley J. D., Rotenberg E., Speck F., “Epitaxial graphene: a new material,” *Phys. status solidi*, 7, 1436–1446, Jul. 2008.

- [35]Sprinkle M., Soukiassian P., de Heer W. A., Berger C., Conrad E. H., “Epitaxial graphene: the material for graphene electronics,” *Phys. status solidi - Rapid Res. Lett.*, 6, A91–A94, Sep. 2009.
- [36]Rollings E., Gweon G.-H., Zhou S. Y., Mun B. S., McChesney J. L., Hussain B. S., Fedorov A. V., First P. N., de Heer W. A., Lanzara A., “Synthesis and characterization of atomically thin graphite films on a silicon carbide substrate,” *J. Phys. Chem. Solids*, 9–10, 2172–2177, Sep. 2006.
- [37]Heer W. A. De, Berger C., Wu X., First P. N., Conrad E. H., Li X., Li T., Sprinkle M., Hass J., Sadowski M. L., Potemski M., “Epitaxial graphene,” 92–100, 2007.
- [38]Mattausch A., Pankratov O., “Density functional study of graphene overlayers on SiC,” *Phys. status solidi*, 7, 1425–1435, Jul. 2008.
- [39]Yang X., Dou X., Rouhanipour A., Zhi L., Räder H. J., Müllen K., “Two-dimensional graphene nanoribbons,” *J. Am. Chem. Soc.*, 13, 4216–7, Apr. 2008.
- [40]Carissan Y., Klopper W., “Growing graphene sheets from reactions with methyl radicals: a quantum chemical study,” *Chemphyschem*, 8, 1770–8, Aug. 2006.
- [41]Zhi L., Müllen K., “A bottom-up approach from molecular nanographenes to unconventional carbon materials,” *J. Mater. Chem.*, 13, 1472, 2008.
- [42]Kim C., Min B., Jung W., “Preparation of graphene sheets by the reduction of carbon monoxide,” *Carbon N. Y.*, 6, 1610–1612, May 2009.
- [43]Jiao L., Zhang L., Wang X., Diankov G., Dai H., “Narrow graphene nanoribbons from carbon nanotubes,” *Nature*, 7240, 877–80, Apr. 2009.

- [44]Kosynkin D. V, Higginbotham A. L., Sinitskii A., Lomeda J. R., Dimiev A., Price B. K., Tour J. M., “Longitudinal unzipping of carbon nanotubes to form graphene nanoribbons,” *Nature*, 7240, 872–6, Apr. 2009.
- [45]Hirsch A., “Unzipping carbon nanotubes: a peeling method for the formation of graphene nanoribbons,” *Angew. Chem. Int. Ed. Engl.*, 36, 6594–6, Jan. 2009.
- [46] Maneechakr, P., & Mongkollertlop, S. (2020). Investigation on adsorption behaviors of heavy metal ions (Cd^{2+} , Cr^{3+} , Hg^{2+} and Pb^{2+}) through low-cost/active manganese dioxide-modified magnetic biochar derived from palm kernel cake residue. *Journal of Environmental Chemical Engineering*, 8(6), 104467.
- [47]Kim H., Abdala A. a., Macosko C. W., “Graphene/Polymer Nanocomposites,” *Macromolecules*, 16, 6515–6530, Aug. 2010.
- [48]Worsley K. A., Ramesh P., Mandal S. K., Niyogi S., Itkis M. E., Haddon R. C., “Soluble graphene derived from graphite fluoride,” *Chem. Phys. Lett.*, 1–3, 51–56, Sep. 2007.
- [49]Chen G., Wu D., Weng W., Wu C., “Exfoliation of graphite flake and its nanocomposites,” *Carbon N. Y.*, 579–625, 2003.
- [50]Carr K. E., “AND OXIDATION EFFECTS ON GRAPHITE OF A MIXTURE OF SULPHURIC,” 1969.
- [51]Lee J. H., Shin D. W., Makotchenko V. G., Nazarov A. S., Fedorov V. E., Kim Y. H., Choi J., Kim J. M., Yoo J., “One-Step Exfoliation Synthesis of Easily Soluble Graphite and Transparent Conducting Graphene Sheets,” *Adv. Mater.*, 43, 4383–4387, Nov. 2009.

[52]Kalaitzidou K., Fukushima H., Drzal L. T., “A new compounding method for exfoliated graphite–polypropylene nanocomposites with enhanced flexural properties and lower percolation threshold,” *Compos. Sci. Technol.*, 10, 2045–2051, Aug. 2007.

[53]Kalaitzidou K., Fukushima H., Askeland P., Drzal L. T., “The nucleating effect of exfoliated graphite nanoplatelets and their influence on the crystal structure and electrical conductivity of polypropylene nanocomposites,” *J. Mater. Sci.*, 8, 2895–2907, Oct. 2007.

[54]Novoselov K. S., Geim A. K., Morozov S. V, Jiang D., Zhang Y., Dubonos S. V, Grigorieva I. V, Firsov A. A., “Electric field effect in atomically thin carbon films.,” *Science*, 5696, 666–9, Oct. 2004.

[55]Bourlinos A. B., Georgakilas V., Zboril R., Steriotis T. A., Stubos A. K., “Liquid-phase exfoliation of graphite towards solubilized graphenes.,” *Small*, 16, 1841–5, Aug. 2009.

[56]Hernandez Y., Nicolosi V., Lotya M., Blighe F. M., Sun Z., De S., McGovern I. T., Holland B., Byrne M., Gun’Ko Y. K., Boland J. J., Niraj P., Duesberg G., Krishnamurthy S., Goodhue R., Hutchison J., Scardaci V., Ferrari A. C., Coleman J. N., “High-yield production of graphene by liquid-phase exfoliation of graphite.,” *Nat. Nanotechnol.*, 9, 563–8, Sep. 2008.

[57]Liu N., Luo F., Wu H., Liu Y., Zhang C., Chen J., “One-Step Ionic-Liquid-Assisted Electrochemical Synthesis of Ionic-Liquid-Functionalized Graphene Sheets Directly from Graphite,” *Adv. Funct. Mater.*, 10, 1518–1525, May 2008.

[58]Behabtu N., Lomeda J. R., Green M. J., Higginbotham A. L., Sinitskii A., Kosynkin D. V, Tsentelovich D., Parra-Vasquez A. N. G., Schmidt J., Kesselman E., Cohen Y., Talmon Y., Tour J. M., Pasquali M., “Spontaneous high-concentration dispersions and liquid crystals of graphene.,” *Nat. Nanotechnol.*, 6, 406–11, Jun. 2010.

- [59] Brodie B. C., "On the Atomic Weight of Graphite," *Philos. Trans. R. Soc. London*, January, 249–259, Jan. 1859.
- [60] Staudenmaier L., "graphie oxie preparation," *Ber. Dtsch. Chem. Ges*, 1481–1487, 1898.
- [61] Hummers W. S., Offeman R. E., "Preparation of Graphitic Oxide," *J. Am. Chem. Soc.*, 6, 1339–1339, Mar. 1958.
- [62] Park S., Ruoff R. S., "Chemical methods for the production of graphenes.," *Nat. Nanotechnol.*, 4, 217–24, Apr. 2009.
- [63] Boukhvalov D. W., Katsnelson M. I., "Modeling of graphite oxide.," *J. Am. Chem. Soc.*, 32, 10697–701, Aug. 2008.
- [64] Gao W., Alemany L. B., Ci L., Ajayan P. M., "New insights into the structure and reduction of graphite oxide.," *Nat. Chem.*, 5, 403–8, Aug. 2009.
- [65] Jeong H., Lee Y. P., Lahaye R. J. W. E., Park M.-H., An K. H., Kim I. J., Yang C., Park C. Y., Ruoff R. S., Lee Y. H., "Evidence of graphitic AB stacking order of graphite oxides.," *J. Am. Chem. Soc.*, 4, 1362–6, Jan. 2008.
- [66] Cai W., Piner R. D., Stadermann F. J., Park S., Shaibat M. A., Ishii Y., Yang D., Velamakanni A., An S. J., Stoller M., An J., Chen D., Ruoff R. S., "Synthesis and solid-state NMR structural characterization of ^{13}C -labeled graphite oxide.," *Science*, 5897, 1815–7, Sep. 2008.
- [67] Wang S., Sun H., Ang H. M., Tadé M. O., "Adsorptive remediation of environmental pollutants using novel graphene-based nanomaterials," *Chem. Eng. J.*, 336–347, Jun. 2013.

- [68]Stankovich S., Dikin D. A., Piner R. D., Kohlhaas K. A., Kleinhammes A., Jia Y., Wu Y., Nguyen S. T., Ruoff R. S., “Synthesis of graphene-based nanosheets via chemical reduction of exfoliated graphite oxide,” *Carbon N. Y.*, 7, 1558–1565, Jun. 2007.
- [69]Wang G., Shen X., Wang B., Yao J., Park J., “Synthesis and characterisation of hydrophilic and organophilic graphene nanosheets,” *Carbon N. Y.*, 5, 1359–1364, Apr. 2009.
- [70]Lomeda J. R., Doyle C. D., Kosynkin D. V., Hwang W., Tour J. M., “Diazonium functionalization of surfactant-wrapped chemically converted graphene sheets,” *J. Am. Chem. Soc.*, 48, 16201–6, Dec. 2008.
- [71]Si Y., Samulski E. T., “Synthesis of water soluble graphene,” *Nano Lett.*, 6, 1679–82, Jun. 2008.
- [72]Wang G., Yang J., Park J., Gou X., Wang B., Liu H., Yao J., “Facile Synthesis and Characterization of Graphene Nanosheets,” *J. Phys. Chem. C*, 22, 8192–8195, Jun. 2008.
- [73]Williams G., Seger B., Kamat P. V., “TiO₂-graphene nanocomposites. UV-assisted photocatalytic reduction of graphene oxide,” *ACS Nano*, 7, 1487–91, Jul. 2008.
- [74]Zhou Y., Bao Q., Tang L. A. L., Zhong Y., Loh K. P., “Hydrothermal Dehydration for the ‘Green’ Reduction of Exfoliated Graphene Oxide to Graphene and Demonstration of Tunable Optical Limiting Properties,” *Chem. Mater.*, 13, 2950–2956, Jul. 2009.
- [75]Fan Z., Wang K., Wei T., Yan J., Song L., Shao B., “An environmentally friendly and efficient route for the reduction of graphene oxide by aluminum powder,” *Carbon N. Y.*, 5, 1686–1689, Apr. 2010.

- [76]McAllister M. J., Li J., Adamson D. H., Schniepp H. C., Abdala A. A., Liu J., Herrera-Alonso M., Milius D. L., Car R., Prud'homme R. K., Aksay I. A., "Single Sheet Functionalized Graphene by Oxidation and Thermal Expansion of Graphite," *Chem. Mater.*, 18, 4396–4404, Sep. 2007.
- [77]Schniepp H. C., Li J., McAllister M. J., Sai H., Herrera-Alonso M., Adamson D. H., Prud'homme R. K., Car R., Saville D. A., Aksay I. A., "Functionalized single graphene sheets derived from splitting graphite oxide.," *J. Phys. Chem. B*, 17, 8535–9, May 2006.
- [78]Du X., Skachko I., Barker A., Andrei E. Y., "Approaching ballistic transport in suspended graphene.," *Nat. Nanotechnol.*, 8, 491–5, Aug. 2008.
- [79]Park M. J., Lee J. K., Lee B. S., Lee Y.-W., Choi I. S., Lee S., "Covalent Modification of Multiwalled Carbon Nanotubes with Imidazolium-Based Ionic Liquids: Effect of Anions on Solubility," *Chem. Mater.*, 6, 1546–1551, Mar. 2006.
- [80]Fang M., Wang K., Lu H., Yang Y., Nutt S., "Single-layer graphene nanosheets with controlled grafting of polymer chains," *J. Mater. Chem.*, 10, 1982, 2010.
- [81]Bourlinos A. B., Gournis D., Petridis D., Szabó T., Szeri A., Dékány I., "Graphite Oxide: Chemical Reduction to Graphite and Surface Modification with Primary Aliphatic Amines and Amino Acids," *Langmuir*, 15, 6050–6055, Jul. 2003.
- [82]Lotya M., Hernandez Y., King P. J., Smith R. J., Nicolosi V., Karlsson L. S., Blighe F. M., De S., Wang Z., McGovern I. T., Duesberg G. S., Coleman J. N., "Liquid phase production of graphene by exfoliation of graphite in surfactant/water solutions.," *J. Am. Chem. Soc.*, 10, 3611–20, Mar. 2009.

- [83]Hamilton C. E., Lomeda J. R., Sun Z., Tour J. M., Barron A. R., “High-yield organic dispersions of unfunctionalized graphene.” *Nano Lett.*, 10, 3460–2, Oct. 2009.
- [84]Kuila T., Bose S., Mishra A. K., Khanra P., Kim N. H., Lee J. H., “Chemical functionalization of graphene and its applications,” *Prog. Mater. Sci.*, 7, 1061–1105, Sep. 2012.
- [85]Kuila T., Bose S., Hong C. E., Uddin M. E., Khanra P., Kim N. H., Lee J. H., “Preparation of functionalized graphene/linear low density polyethylene composites by a solution mixing method,” *Carbon N. Y.*, 3, 1033–1037, Mar. 2011.
- [86]Shan C., Yang H., Han D., Zhang Q., Ivaska A., Niu L., “Water-Soluble Graphene Covalently Functionalized by Biocompatible,” 26, 15343–15346, 2009.
- [87]Bekyarova E., Itkis M. E., Ramesh P., Berger C., Sprinkle M., de Heer W. A., Haddon R. C., “Chemical modification of epitaxial graphene: spontaneous grafting of aryl groups,” *J. Am. Chem. Soc.*, 4, 1336–7, Feb. 2009.
- [88]Stankovich S., Piner R. D., Nguyen S. T., Ruoff R. S., “Synthesis and exfoliation of isocyanate-treated graphene oxide nanoplatelets,” *Carbon N. Y.*, 15, 3342–3347, Dec. 2006.
- [89]Stankovich S., Dikin D. A., Dommett G. H. B., Kohlhaas K. M., Zimney E. J., Stach E. A., Piner R. D., Nguyen S. T., Ruoff R. S., “Graphene-based composite materials,” *Nature*, 7100, 282–6, Jul. 2006.
- [90]Zhang D., Zu S., Han B., “Inorganic–organic hybrid porous materials based on graphite oxide sheets,” *Carbon N. Y.*, 13, 2993–3000, Nov. 2009.

- [91]Hu H., Wang X., Wang J., Liu F., Zhang M., Xu C., “Microwave-assisted covalent modification of graphene nanosheets with chitosan and its electrorheological characteristics,” *Appl. Surf. Sci.*, 7, 2637–2642, Jan. 2011.
- [92]Choi J., Kim K., Kim B., Lee H., Kim S., “Covalent Functionalization of Epitaxial Graphene by Azidotrimethylsilane,” *J. Phys. Chem. C*, 22, 9433–9435, Jun. 2009.
- [93]Georgakilas V., Bourlinos A. B., Zboril R., Steriotis T. a, Dallas P., Stubos A. K., Trapalis C., “Organic functionalisation of graphenes.,” *Chem. Commun. (Camb)*, 10, 1766–8, Mar. 2010.
- [94]Zhao Y.-L., Stoddart J. F., “Noncovalent functionalization of single-walled carbon nanotubes.,” *Acc. Chem. Res.*, 8, 1161–71, Aug. 2009.
- [95]Nakayama-Ratchford N., Bangsaruntip S., Sun X., Welsher K., Dai H., “Noncovalent functionalization of carbon nanotubes by fluorescein-polyethylene glycol: supramolecular conjugates with pH-dependent absorbance and fluorescence.,” *J. Am. Chem. Soc.*, 9, 2448–9, Mar. 2007.
- [96]Stankovich S., Piner R. D., Chen X., Wu N., Nguyen S. T., Ruoff R. S., “Stable aqueous dispersions of graphitic nanoplatelets via the reduction of exfoliated graphite oxide in the presence of poly(sodium 4-styrenesulfonate),” *J. Mater. Chem.*, 2, 155, 2006.
- [97]Bai H., Xu Y., Zhao L., Li C., Shi G., “Non-covalent functionalization of graphene sheets by sulfonated polyaniline.,” *Chem. Commun. (Camb)*, 13, 1667–9, Apr. 2009.
- [98]Xu Y., Bai H., Lu G., Li C., Shi G., “Flexible graphene films via the filtration of water-soluble noncovalent functionalized graphene sheets.,” *J. Am. Chem. Soc.*, 18, 5856–7, May 2008.

- [99]Choi E., Han T. H., Hong J., Kim J. E., Lee S. H., Kim H. W., Kim S. O., “Noncovalent functionalization of graphene with end-functional polymers,” *J. Mater. Chem.*, 10, 1907, 2010.
- [100]Liu J., Yang W., Tao L., Li D., Boyer C., Davis T. P., “Thermosensitive graphene nanocomposites formed using pyrene-terminal polymers made by RAFT polymerization,” *J. Polym. Sci. Part A Polym. Chem.*, 2, 425–433, Jan. 2010.
- [101]Yang H., Zhang Q., Shan C., Li F., Han D., Niu L., “Stable, conductive supramolecular composite of graphene sheets with conjugated polyelectrolyte,” *Langmuir*, 9, 6708–12, May 2010.
- [102]Park S., An J., Piner R. D., Jung I., Yang D., Velamakanni A., Nguyen S. T., Ruoff R. S., “Aqueous Suspension and Characterization of Chemically Modified Graphene Sheets,” *Chem. Mater.*, 21, 6592–6594, Nov. 2008.
- [103]Li D., Müller M. B., Gilje S., Kaner R. B., Wallace G. G., “Processable aqueous dispersions of graphene nanosheets,” *Nat. Nanotechnol.*, 2, 101–5, Feb. 2008.
- [104]Kim K. S., Zhao Y., Jang H., Lee S. Y., Kim J. M., Kim K. S., Ahn J., Kim P., Choi J., Hong B. H., “Large-scale pattern growth of graphene films for stretchable transparent electrodes,” *Nature*, 7230, 706–710, 2008.
- [105]Hao R., Qian W., Zhang L., Hou Y., “Aqueous dispersions of TCNQ-anion-stabilized graphene sheets,” *Chem. Commun. (Camb)*, 48, 6576–8, Dec. 2008.
- [106]Ansari S., Giannelis E. P., “Functionalized graphene sheet-Poly(vinylidene fluoride) conductive nanocomposites,” *J. Polym. Sci. Part B Polym. Phys.*, 9, 888–897, May 2009.

- [107]Zhang H., Zheng W., Yan Q., Yang Y., Wang J., Lu Z., Ji G., Yu Z., “Electrically conductive polyethylene terephthalate / graphene nanocomposites prepared by melt compounding,” *Polymer (Guildf)*, 5, 1191–1196, 2010.
- [108]Kim H., Thomas Hahn H., Viculis L. M., Gilje S., Kaner R. B., “Electrical conductivity of graphite/polystyrene composites made from potassium intercalated graphite,” *Carbon N. Y.*, 7, 1578–1582, Jun. 2007.
- [109]Zheng W., Lu X., Wong S., “Electrical and mechanical properties of expanded graphite-reinforced high-density polyethylene,” *J. Appl. Polym. Sci.*, 5, 2781–2788, Mar. 2004.
- [110]Ye L., Meng X., Ji X., Li Z., Tang J., “Synthesis and characterization of expandable graphite–poly(methyl methacrylate) composite particles and their application to flame retardation of rigid polyurethane foams,” *Polym. Degrad. Stab.*, 6, 971–979, Jun. 2009.
- [111]Lee W. D., Im S. S., “Thermomechanical properties and crystallization behavior of layered double hydroxide/poly(ethylene terephthalate) nanocomposites prepared by in-situ polymerization,” *J. Polym. Sci. Part B Polym. Phys.*, 1, 28–40, Jan. 2007.
- [112]Hussain F., “Review article: Polymer-matrix Nanocomposites, Processing, Manufacturing, and Application: An Overview,” *J. Compos. Mater.*, 17, 1511–1575, Jan. 2006.
- [113]Liang J., Huang Y., Zhang L., Wang Y., Ma Y., Guo T., Chen Y., “Molecular-Level Dispersion of Graphene into Poly(vinyl alcohol) and Effective Reinforcement of their Nanocomposites,” *Adv. Funct. Mater.*, 14, 2297–2302, Jul. 2009.

- [114] Lee J., Kim S. K., Kim N. H., “Effects of the addition of multi-walled carbon nanotubes on the positive temperature coefficient characteristics of carbon-black-filled high-density polyethylene nanocomposites,” *Scr. Mater.*, 12, 1119–1122, Dec. 2006.
- [115] Kalaitzidou K., Fukushima H., Drzal L. T., “Mechanical properties and morphological characterization of exfoliated graphite–polypropylene nanocomposites,” *Compos. Part A Appl. Sci. Manuf.*, 7, 1675–1682, Jul. 2007.
- [116] Kim S., Do I., Drzal L. T., “Thermal stability and dynamic mechanical behavior of exfoliated graphite nanoplatelets-LLDPE nanocomposites,” *Polym. Compos.*, 5, 755–761, Jan. 2009.
- [117] Weng W., Chen G., Wu D., “Transport properties of electrically conducting nylon 6/foiled graphite nanocomposites,” *Polymer (Guildf.)*, 16, 6250–6257, Jul. 2005.
- [118] Bourlinos A. B., Gournis D., Petridis D., Szabó T., Szeri A., Dékány I., “Graphite Oxide: Chemical Reduction to Graphite and Surface Modification with Primary Aliphatic Amines and Amino Acids,” *Langmuir*, 15, 6050–6055, Jul. 2003.
- [119] Dashtian K, Zare-Dorabei R. An easily organic–inorganic hybrid optical sensor based on dithizone impregnation on mesoporous SBA-15 for simultaneous detection and removal of Pb²⁺ ions from water samples: response-surface methodology. *Appl Organomet Chem.* 2017;12(31):1–14.
- [120] Mahar FK, He L, Wei K, Mehdi M, Zhu M, Gu J, et al. Rapid adsorption of lead ions using porous carbon nanofibers. *Chemosphere.* 2019;225:360–7.

- [121]. Chen Q, Yao Y, Li X, Lu J, Zhou J, Huang Z. Comparison of heavy metal removals from aqueous solutions by chemical precipitation and characteristics of precipitates. *J Water Proc Eng.* 2018;26:289–300.
- [122]. Vajedi F, Dehghani H. The characterization of TiO₂-reduced graphene oxide nanocomposites and their performance in electrochemical determination for removing heavy metals ions of cadmium(II), lead(II) and copper(II). *Mater Sci Eng B.* 2019;243:189–98.
- [123]. Nekouei RK, Pahlevani F, Assefi M, Maroufi S, Sahajwalla V. Selective isolation of heavy metals from spent electronic waste solution by macroporous ion-exchange resins. *J Hazard Mater.* 2019;371:389–96.
- [124]. Ma A, Abushaikha A, Allen SJ, Mckay G. Ion exchange homogeneous surface diffusion modelling by binary site resin for the removal of nickel ions from wastewater in fixed beds. *Chem Eng J.* 2019;358:1–10.
- [125]. Al-Senani GM, Al-Fawzan FF. Adsorption study of heavy metal ions from aqueous solution by nanoparticle of wild herbs. *Egyptian J Aquatic Res.* 2018;44:187–94.
- [126]. Xin J, Tang J, Liu Y, Zhang Y, Tian R. Pre-aeration of the rhizosphere offers potential for phytoremediation of heavy metal-contaminated wetlands. *J Hazard Mater.* 2019;374:437–46.
- [127]. Kyzas GZ, Bomis G, Kosheleva RI, Efthimiadou EK, Favvas EP, Kostoglou M, et al. Nanobubbles effect on heavy metal ions adsorption by activated carbon. *Chem Eng J.* 2019;356:91–7.
- [128] Tadjarodi A, Moazen Ferdowsi S, Zare-Dorabei R, Barzin A. Highly efficient ultrasonic-assisted removal of Hg(II) ions on graphene oxide modified with 2-pyridinecarboxaldehyde

thiosemicarbazone: adsorption isotherms and kinetics studies. *Ultrason Sonochem.* 2016;33:118–28.

[130] S. Velusamy, A. Roy, S. Sundaram, T. Kumar Mallick, A Review on Heavy Metal Ions and Containing Dyes Removal Through Graphene Oxide-Based Adsorption Strategies for Textile Wastewater Treatment. *Chem. Rec.* 2021, 21, 1570.

[131].Tollefson J., Gilbert N., “Earth summit: Rio report card.,” *Nature*, 7401, 20–3, Jun. 2012.

[132].Khor E., “Chitin: Fulfilling a Biomaterials Promise.”2001.

[133].Ravi Kumar M. N. ., “A review of chitin and chitosan applications,” *React. Funct. Polym.*, 1, 1–27, Nov. 2000.

[134].Geim A. K., Novoselov K. S., “The rise of graphene.,” *Nat. Mater.*, 3, 183–91, Mar. 2007.

[135].Singh V., Joung D., Zhai L., Das S., Khondaker S. I., Seal S., “Graphene based materials: Past, present and future,” *Prog. Mater. Sci.*, 8, 1178–1271, Oct. 2011.

[136]. Zhang, M., Zhao, F., Li, H., Dong, S., Yang, Y., Hou, X., ... & Jiang, Z. (2021). Ferrocene functionalized graphene: preparation, characterization and application as an efficient catalyst for the thermal decomposition of TKX-50. *Physical Chemistry Chemical Physics*, 23(32), 17567-17575.

[137]. Georgakilas, V., Otyepka, M., Bourlinos, A. B., Chandra, V., Kim, N., Kemp, K. C., ... & Kim, K. S. (2012). Functionalization of graphene: covalent and non-covalent approaches, derivatives and applications. *Chemical reviews*, 112(11), 6156-6214.

- [138]. Wang, X., Wang, W., Liu, Y., Ren, M., Xiao, H., & Liu, X. (2016). Characterization of conformation and locations of C–F bonds in graphene derivative by polarized ATR-FTIR. *Analytical chemistry*, 88(7), 3926-3934.
140. Alyasi, H., Mackey, H.R. & McKay, G. Comparison of Cadmium Adsorption from Water Using Same Source Chitosan and Nanochitosan: Is It Worthwhile to Go Nano?. *J Polym Environ* **30**, 2727–2738 (2022). <https://doi.org/10.1007/s10924-021-02344-7>.
141. Srivastava VC, Indra Deo Mall ID, Misra M (2006) Equilibrium modelling of single and binary adsorption of cadmium and nickel onto bagasse ash. *Chem Eng J* 117:79–91.
142. Boparai HK, Joseph M, O’Carroll DM (2013) Cadmium (Cd²⁺) removal by nano zerovalent iron: Surface analysis, effects of solution chemistry and surface complexation modelling. *Environ Sci Poll Res* 20:6210–6221.
143. Lehman RG, Harter RD (1984) Assessment of copper–soil bond strength by desorption kinetics. *Soil Sci Soc Am J* 48:769–772.
144. Langmuir I (1916) The constitution and fundamental properties of solids and liquids. *J Am Chem Soc* 38:2221–2295.
145. Kalavathy MH, Miranda LR (2010) A solid phase extractant for the removal of copper, nickel and zinc from aqueous solutions. *Chem Eng J* 158:188–199.
146. Ho YS, McKay G (1998) A comparison of chemisorption kinetic models applied to pollutant removal on various sorbents. *Proc Saf Environ Prot* 6:332–340.
147. Mahmoud, Z. H., Mahdi, A. B., Alnassar, Y. S., & AL-Salman, H. N. K. (2023). Formulation and Sustained-Release of Verapamil Hydrochloride Tablets. *The Chemist*, 76.

148. Al-Obaidi, N. S., Sadeq, Z. E., Mahmoud, Z. H., Abd, A. N., Al-Mahdawi, A. S., & Ali, F. K. (2023). Synthesis of Chitosan-TiO₂ Nanocomposite for Efficient Cr (VI) Removal from Contaminated Wastewater Sorption Kinetics, Thermodynamics and Mechanism. *Journal of Oleo Science*, 72(3), 337-346.

149. Jasim, S. A., Jabbar, A. H., Bokov, D. O., Al Mashhadani, Z. I., Surendar, A., Taban, T. Z., ... & Mustafa, Y. F. (2023). The Effects of Oxide Layer on the Joining Performance of CuZr Metallic Glasses. *Transactions of the Indian Institute of Metals*, 76(1), 239-247.

150. Jasim, S. A., Ali, M. H., Mahmood, Z. H., Rudiansyah, M., Alsultany, F. H., Mustafa, Y. F., ... & Surendar, A. (2022). Role of Alloying Composition on Mechanical Properties of CuZr Metallic Glasses During the Nanoindentation Process. *Metals and Materials International*, 28(9), 2075-2082.

151. Bokov, D. O., Mustafa, Y. F., Mahmoud, Z. H., Suksatan, W., Jawad, M. A., & Xu, T. (2022). Cr-SiNT, Mn-SiNT, Ti-C70 and Sc-CNT as Effective Catalysts for CO₂ Reduction to CH₃OH. *Silicon*, 14(14), 8493-8503.

152. Jasim, S. A., Abdelbasset, W. K., Hachem, K., Kadhim, M. M., Yasin, G., Obaid, M. A., ... & Mahmoud, Z. H. (2022). Novel Gd₂O₃/SrFe₁₂O₁₉@ Schiff base chitosan (Gd/SrFe@ SBCs) nanocomposite as a novel magnetic sorbent for the removal of Pb (II) and Cd (II) ions from aqueous solution. *Journal of the Chinese Chemical Society*, 69(7), 1079-1087.

153. Mansoor Al Sarraf, A. A., H. Alsultany, F., H. Mahmoud, Z., S. Shafik, S., Al Mashhadani, Z. I., & Sajjadi, A. (2022). Magnetic nanoparticles supported zinc (II) complex (Fe₃O₄@ SiO₂-Imine/Thio-Zn (OAc)₂): a green and efficient magnetically reusable zinc nanocatalyst for

synthesis of nitriles via cyanation of aryl iodides. *Synthetic Communications*, 52(9-10), 1245-1253.

154.Hameed Mahmood, Z., Riadi, Y., Hammoodi, H. A., Alkaim, A. F., & Fakri Mustafa, Y. (2022). Magnetic Nanoparticles Supported Copper Nanocomposite: A Highly Active Nanocatalyst for Synthesis of Benzothiazoles and Polyhydroquinolines. *Polycyclic Aromatic Compounds*, 1-19.

155.Mahmoud, Z. H., AL-Bayati, R. A., & Khadom, A. A. (2022). The efficacy of samarium loaded titanium dioxide (Sm: TiO₂) for enhanced photocatalytic removal of rhodamine B dye in natural sunlight exposure. *Journal of Molecular Structure*, 1253, 132267.

156.Raya, I., Mansoor Al Sarraf, A. A., Widjaja, G., Ghazi Al-Shawi, S., F Ramadan, M., Mahmood, Z. H., ... & Ghaleb Maabreh, H. (2022). ZnMoO₄ Nanoparticles: Novel and Facile Synthesis, Characterization, and Photocatalytic Performance. *Journal of Nanostructures*, 12(2), 446-454.

157.Mahmood, Z. H., Jarosova, M., Kzar, H. H., Machek, P., Zaidi, M., Dehno Khalaji, A., ... & Kadhim, M. M. (2022). Synthesis and characterization of Co₃O₄ nanoparticles: Application as performing anode in Li-ion batteries. *Journal of the Chinese Chemical Society*, 69(4), 657-662.

158.Mahmoud, Z. H., AL-Bayati, R. A., & Khadom, A. A. (2022). Electron transport in dye-sanitized solar cell with tin-doped titanium dioxide as photoanode materials. *Journal of Materials Science: Materials in Electronics*, 33(8), 5009-5023.

159. Bahadoran, A., Jabarabadi, M. K., Mahmood, Z. H., Bokov, D., Janani, B. J., & Fakhri, A. (2022). Quick and sensitive colorimetric detection of amino acid with functionalized-silver/copper nanoparticles in the presence of cross linker, and bacteria detection by using DNA-template nanoparticles as peroxidase activity. *Spectrochimica Acta Part A: Molecular and Biomolecular Spectroscopy*, 268, 120636.
160. Smaisim, G.F., Abed, A.M., Al-Madhhachi, H. *et al.* Graphene-Based Important Carbon Structures and Nanomaterials for Energy Storage Applications as Chemical Capacitors and Supercapacitor Electrodes: a Review. *BioNanoSci.* **13**, 219–248 (2023). <https://doi.org/10.1007/s12668-022-01048-z>.
161. Kadhim, M. M., Rheima, A. M., Abbas, Z. S., Jlood, H. H., Hachim, S. K., & Kadhum, W. R. (2023). Evaluation of a biosensor-based graphene oxide-DNA nanohybrid for lung cancer. *RSC Advances*, 13(4), 2487-2500.
162. Salahdin, O. D., Sayadi, H., Solanki, R., Parra, R. M. R., Al-Thamir, M., Jalil, A. T., ... & Kianfar, E. (2022). Graphene and carbon structures and nanomaterials for energy storage. *Applied Physics A*, 128(8), 703.
163. Abdelbasset, W. K., Jasim, S. A., Bokov, D. O., Oleneva, M. S., Islamov, A., Hammid, A. T., ... & Kianfar, E. (2022). Comparison and evaluation of the performance of graphene-based biosensors. *Carbon Letters*, 32(4), 927-951.
164. Bokov, D., Turki Jalil, A., Chupradit, S., Suksatan, W., Javed Ansari, M., Shewael, I. H., ... & Kianfar, E. (2021). Nanomaterial by sol-gel method: synthesis and application. *Advances in Materials Science and Engineering*, 2021, 1-21.

165. Kyzas, G. Z., Lazaridis, N. K., & Kostoglou, M. (2012). Modelling the effect of pre-swelling on adsorption dynamics of dyes by chitosan derivatives. *Chemical engineering science*, 81, 220-230.
166. Qiao, L., Wang, S., Wang, T. *et al.* High-strength and low-swelling chitosan/cellulose microspheres as a high-efficiency adsorbent for dye removal. *Cellulose* **28**, 9323–9333 (2021). <https://doi.org/10.1007/s10570-021-04111-2>.
167. Ruiz, M., Sastre, A.M., Guibal, E., 2000. Palladium sorption on glutaraldehyde crosslinked chitosan. *React. Funct. Polym.* 45, 155–173. [https://doi.org/10.1016/S1381-5148\(00\)00019-5](https://doi.org/10.1016/S1381-5148(00)00019-5).
168. Chang, Y.-C., Chang, S.-W., Chen, D.-H., 2006. Magnetic chitosan nanoparticles: studies on chitosan binding and adsorption of Co(II) ions. *React. Funct. Polym.* 66, 335–341. <https://doi.org/10.1016/j.reactfunctpolym.2005.08.006>.
169. Zhou, L., Xu, J., Liang, X., Liu, Z., 2010. Adsorption of platinum(IV) and palladium(II) from aqueous solution by magnetic cross-linking chitosan nanoparticles modified with ethylenediamine. *J. Hazard Mater.* 182, 518–524. <https://doi.org/10.1016/j.jhazmat.2010.06.062>.
170. Zhang, Yuzhe, Bian, T., Jiang, R., Zhang, Yi, Zheng, X., Li, Z., 2021. Bionic chitosan carbon imprinted aerogel for high selective recovery of Gd(III) from end-of-life rare earth productions. *J. Hazard Mater.* 407, 124347. <https://doi.org/10.1016/j.jhazmat.2020.124347>.
171. Cheng, Q., Zhang, Y., Zheng, X., Sun, W., Li, B., Wang, D., Li, Z., 2021. High specific surface crown ether modified chitosan nanofiber membrane by low-temperature phase separation

for efficient selective adsorption of lithium. *Separ. Purif. Technol.* 262, 118312. <https://doi.org/10.1016/j.seppur.2021.118312>.

172. Tirtom, V.N., Dinçer, A., Becerik, S., Aydemir, T., Çelik, A., 2012. Comparative adsorption of Ni(II) and Cd(II) ions on epichlorohydrin crosslinked chitosan–clay composite beads in aqueous solution. *Chem. Eng. J.* 197, 379–386. <https://doi.org/10.1016/j.cej.2012.05.059>.

173. Mohamed, R.R., Elella, M.H.A., Sabaa, M.W., 2017. Cytotoxicity and metal ions removal using antibacterial biodegradable hydrogels based on N -quaternized chitosan/poly (acrylic acid). *Int. J. Biol. Macromol.* 98, 302–313. <https://doi.org/10.1016/j.ijbiomac.2017.01.107>.

174. Yu, Z., Dang, Q., Liu, C., Cha, D., Zhang, H., Zhu, W., Zhang, Q., Fan, B., 2017b. Preparation and characterization of poly(maleic acid)-grafted cross-linked chitosan microspheres for Cd(II) adsorption. *Carbohydr. Polym.* 172, 28–39. <https://doi.org/10.1016/j.carbpol.2017.05.039>.

175. Sutirman, Z.A., Rahim, E.A., Sanagi, M.M., Abd Karim, K.J., Wan Ibrahim, W.A., 2020. New efficient chitosan derivative for Cu(II) ions removal: characterization and adsorption performance. *Int. J. Biol. Macromol.* 153, 513–522. <https://doi.org/10.1016/j.ijbiomac.2020.03.015>.

176. Pal, P., Pal, A., 2019. Treatment of real wastewater: kinetic and thermodynamic aspects of cadmium adsorption onto surfactant-modified chitosan beads. *Int. J. Biol. Macromol.* 131, 1092–1100. <https://doi.org/10.1016/j.ijbiomac.2019.03.121>.

177. Zhang, H., Tan, X., Qiu, T., Zhou, L., Li, R., Deng, Z., 2019a. A novel and biocompatible Fe₃O₄ loaded chitosan polyelectrolyte nanoparticles for the removal of Cd²⁺ ion. *Int. J. Biol. Macromol.* 141, 1165–1174. <https://doi.org/10.1016/j.ijbiomac.2019.09.040>.

178. Tang, S., Yang, J., Lin, L., Peng, K., Chen, Y., Jin, S., Yao, W., 2020. Construction of physically crosslinked chitosan/sodium alginate/calcium ion double-network hydrogel and its application to heavy metal ions removal. *Chem. Eng. J.* 393, 124728. <https://doi.org/10.1016/j.cej.2020.124728>.

179. Kumar, R., Bhattacharya, S., & Sharma, P. (2021). Novel insights into adsorption of heavy metal ions using magnetic graphene composites. *Journal of Environmental Chemical Engineering*, 9(5), 106212.

[180]. A. Jana, E. Scheer, S. Polarz, Synthesis of graphene–transition metal oxide hybrid nanoparticles and their application in various fields, *Beilstein J. Nanotechnol.* 8 (2017) 688–714, <https://doi.org/10.3762/bjnano.8.74>.

[181]. J. Xu, Z. Cao, Y. Zhang, Z. Yuan, Z. Lou, X. Xu, X. Wang, A review of functionalized carbon nanotubes and graphene for heavy metal adsorption from water: preparation, application, and mechanism, *Chemosphere* 195 (2018) 351–364, <https://doi.org/10.1016/j.chemosphere.2017.12.061>.

[182]. Behzadi, G., & Fekri, L. (2013). Electrical parameter and permittivity measurement of water samples using the capacitive sensor. *International Journal of Water Resources and Environmental Sciences*, 2(3), 66-75.

[183]. Pour, G. B., Aval, L. F., & Mirzaee, M. (2020). CNTs supercapacitor based on the PVDF/PVA gel electrolytes. *Recent Patents on Nanotechnology*, 14(2), 163-170.

[184]. Behzadi Pour, G., Fekri Aval, L., & Esmaili, P. (2019). Performance of gas nanosensor in 1-4 per cent hydrogen concentration. *Sensor Review*, 39(4), 622-628.

[185]. Aval, L. F. (2019). Influence of oxide film surface morphology and thickness on the properties of gas sensitive nanostructure sensor. *Indian Journal of Pure & Applied Physics (IJPAP)*, 57(10), 743-749.

[186]. Behzadi pour, G., Nazarpour fard, H., Fekri aval, L., & Esmaili, P. (2020). Polyvinylpyridine-based electrodes: sensors and electrochemical applications. *Ionics*, 26, 549-563.

[187]. Fekri, L., Jafari, A., Fekri, S., Shafikhani, A., Vesaghi, M., & Behzadi, G. (2010). Comparison of synthesis and purification of carbon nanotubes by thermal chemical vapor deposition on the nickel-based catalysts: NiSiO₂ and 304-Type stainless steel. *Journal of Applied Sciences*, 10(9), 716-723.

[188]. Avval, Y. F., Pour, G. B., & Aram, M. M. (2022). Fabrication of high efficiency coronavirus filter using activated carbon nanoparticles. *International Nano Letters*, 12(4), 421-426.

[189]. Alabada, R., Kadhim, M. M., sabri Abbas, Z., Rheima, A. M., Altimari, U. S., Dawood, A. H., ... & Kianfar, E. (2023). Investigation of effective parameters in the production of alumina

gel through the sol-gel method. Case Studies in Chemical and Environmental Engineering, 100405.

[190]. sabri Abbas, Z., Kadhim, M. M., Mahdi Rheima, A., jawad al-bayati, A. D., Talib Abed, Z., dashoor Al-Jaafari, F. M., ... & Kianfar, E. (2023). Preparing Hybrid Nanocomposites on the Basis of Resole/Graphene/Carbon Fibers for Investigating Mechanical and Thermal Properties. BioNanoScience, 1-29.

Journal Pre-proof

Declaration of interests

The authors declare that they have no known competing financial interests or personal relationships that could have appeared to influence the work reported in this paper.

Article Title: A study in analytical chemistry of adsorption of heavy metal ions using chitosan/graphene nanocomposites

Corresponding Author: dr ehsan kianfar

Sincerely,

Dr. Ehsan kianfar

Department of Chemical Engineering,

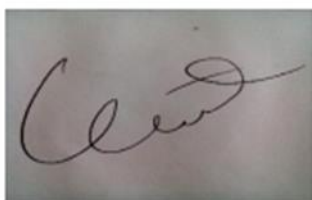
Arak, Branch, Islamic Azad University, Arak,, Iran, P.O. Box: 38135/567, arak, Iran,

Tel: +98-917-7441049, *e-mail: e-kianfar94@iau-arak.ac.ir; ehsan_kianfar2010@yahoo.com.

Home Page: https://scholar.google.com/citations?user=UFP_4q4AAAAJ&hl=en ,

<https://www.researchgate.net/profile/Ehsan-Kianfar-4>.

ORCID:<https://orcid.org/0000-0002-7213-3772>.

A rectangular box containing a handwritten signature in black ink. The signature is cursive and appears to read 'Ehsan Kianfar'. The background of the box is a light, slightly textured grey.